Sudan University of Science and Technology
College of Post-Graduation studies
Mechanical School Production

Optimization of Abrasive Water Jet Cutting Process using Simulation

معيارية عملية القطع بتيار الماء والحبيبات الحاكّة بإستخدام المحاكاة

Thesis submitted to the Postgraduate College Sudan University of Science and Technology in fulfillment of the Requirements for the Degree of M.Sc.

(School Mechanical Engineering-Production Department)

Prepared by:

Abdalla Kamal Abdalla Mohamed

Supervision:

Dr. ELKhawad Ali Elfaki

June 2015

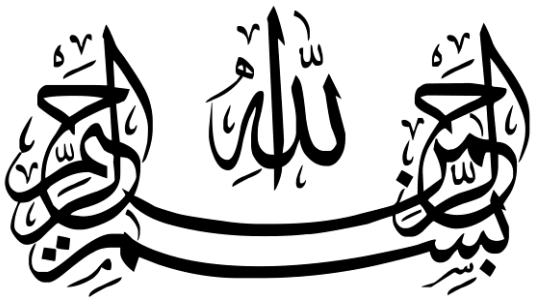

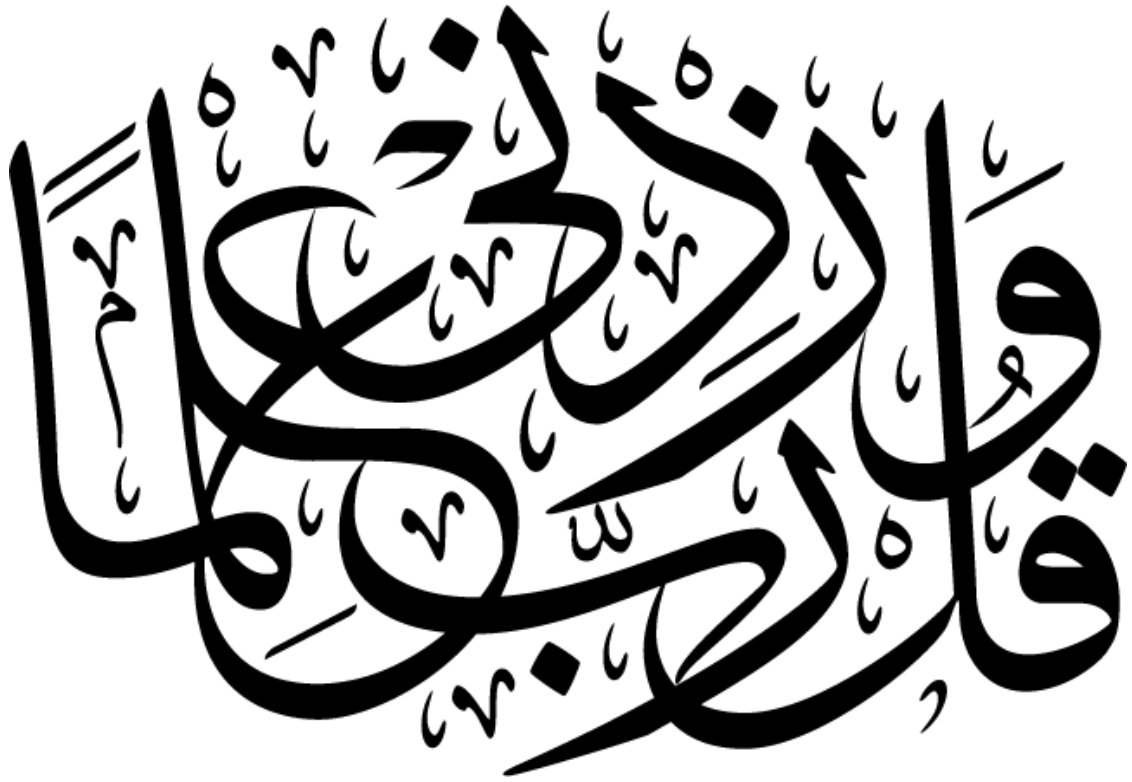

إهداء

إلى كل من أضاء بعلمه عقل غيره

أو هدى بالجواب الصحيح حيرة سائليه

فأظهر بسماحته تواضع العلماء

وبرحابته سماحة العارفين

شكر وتقدير

وللوفاء في قلوبنا مكان

لو أن الشكر يعبّر لمثلكم بالقوافي لانتهت قبل أن ينتهي مثلكم.

ولو أن العرفان يخط بالأقلام لشخصكم لجفت خجلاً قبل أن تكتب اسمكم.

ولكن، يكفينا أن تتوحد الغاية بمعنى جميل عشناه بينكم.

ونسلك الدرب نفسه حتى نصير مثلكم

إلى الأستاذ الغالي: د.الخواض علي الفكي

إلى أهلي وأساتذتي والدي العزيزين وكل من أعانني على إكمال البحث

الى الغالية م.اسراء جعفر مصطفى على الدعم والمساعدة

لكم خالص شكري وتقديري

Abstract

Abrasive Water Jet Machining – (AWJM) become one of popular and growing processes among Advanced Machining Processes. It has high material flexibility and advantages of geometric, and ability to cut materials that are hard to machine using conventional technologies, it reduces the time necessary for secondary operations like programming, tool changing, or clamping. this allows a significant optimization of the overall manufacturing process chain. All these Advantages lead to (AWJM) technology to rapidly spreading in many industries. Since this process one of the important Advanced Machining Processes therefor in this research an Explicit Finite Element Analysis (FEA) conducted and (AWJM) Process Parameters (Impact Angle α, Operational pressure P and Traverse Rate T) studied to provide data to Optimize Abrasive water jet machining process. Result showed an increase in Material Removal Rate (MRR) by (1% – 3%) with increasing Water Pressure P by 200MPa and (4% – 5%) approximately with increasing Traverse Rate T by 20m/s, but also showed drawbacks as surface roughness and damage When Impact Angle 90^{O} showed the best results.

الملخص

اصبحت عملية القطع باستخدام تيار الماء والحبيبات الحاكّة Abrasive Water Jet Machining – (AWJM) واحدة من اهم وأشهر العمليات النامية والمتطورة بين عمليات التشغيل المتقدمة. وذلك لما لدى هذه العملية (AWJM) من مرونة عالية وفوائد هندسة، وكذلك قدرتها علي قطع المواد الصلبة والتي يصعب قطعها بالوسائل والتقنيات التقليدية. وايضا ادت عملية (AWJM) الى تقليل الزمن اللازم للعمليات الثانوية المضيعة للزمن كالزمن الضائع في البرمجة وعملية تغيير ادوات القطع والاقلام وزمن الفك والتثبيت وكل ذلك ادى الى تحسين عام في سلسلة عمليات الصناعة مما ادى الى انتشار هذه التقنية بسرعة في العديد من الصناعات وبما أن هذه التقنية تعتبر من عمليات التشغيل المتقدمة ،فقد تم في هذا البحث إجراء دراسة للعوامل المؤثرة على تقنية (AWJM) عن طريق المحاكاة بإستخدام تحليل العناصر المتناهية – Finite Element Analysis (FEA) (زاوية الاصطدام α، الضغط التشغيلي P، معدل الانتقال T) من أجل توفير بيانات كافية لتحقيق معيارية عملية ال (AWJM) ، اظهرت النتائج زيادة في معدل ازالة المادة **(**Material Removal Rate- MRR) بنسبة (1% – 3%) عند زيادة الضغط للماء ب 200MPa و (4% – 5%) تقريبا عند زيادة معدل الانتقال ب 20m\s ، ولكن اظهرت ايضا تراجع في نعومة السطح بينما اظهرت الزاوية 90^{O} افضل النتائج.

Table of Contents

Abstract v

الملخص vi

CHAPTER I 1

1.1 Preface 2

1.2 Problem Statement 2

1.3 Research Importance 2

1.4 Research Objectives 3

1.5 Scope of Research 3

CHAPTER II 4

2.1 Preface 5

2.2 Advanced Machining Processes 5

2.3 Advanced Machining Methods 5

2.3.1 Ultrasonic Machining (USM) principle 6

2.3.2 Laser beam machining (LBM) 7

2.3.3 Electrical Discharge Machining (EDM) 8

2.3.4 Electrical Discharge Wire Machining (EDWM) 9

2.3.5 Chemical Machining (CM) 10

2.3.6 Electrochemical Machining (ECM) 11

2.3.7 Waterjet Machining 12

2.4 Abrasive Waterjet Machining (AWJM) 14

2.4.1 Previous Studies 16

2.5 Finite Element Analysis (FEA) 21

CHAPTER III 26

3.1 Preface 27

3.2 SolidWorks Design Software 27

3.3 ANSYS Software 29

3.3.1 History 29

3.3.2 ANSYS Advantages 30

3.3.3 Products 32

3.3.4 Explicit Dynamics 34

3.4 3D Model Design 35

3.5 Explicit Finite Element Analysis Simulation 36

3.5.1 Simulation Model 36

3.5.2 Simulation Constrains 37

3.5.3 Simulation Procedure 38
CHAPTER IV 42
4.1 FEA Simulation Results: 43
4.2 FEA Simulation Results Comparison 47
CHAPTER V 48
5.1 FEA Simulation Conclusion: 49
5.2 Recommendations: 49
REFERENCES 50
APPENDICES 52

List of Figures

Figure Number	Figure Title	Page Number
(2-1)	Ultrasonic Machining	6
(2-2)	Finished Parts Processed Using USM	7
(2-3)	Laser beam machining	8
(2-4)	Electrical Discharge Machining (EDM)	9
(2-5)	EDM wire machining	10
(2-6)	Chemical Machining	11
(2-7)	Electrochemical Machining (ECM)	12
(2-8)	Waterjet Machining WJM	13
(2-9)	Finished parts with Waterjet Machining 5 axis	14
(2-10)	Process parameters influencing the AWJ cutting process	15
(2-11)	Abrasive Water Jet Machine AWJM	15
(2-12)	Curved-boundary mesh	22
(2-13)	Tapered circular cylinder subjected to tensile loading	24
(3-1)	Vehicle Analysis using ANSYS Mechanical	33
(3-2)	Products Analysis using ANSYS Explicit Dynamics	34
(3-3)	3D Model for Abrasive water jet machine according to AINNOVATIVE INTERNATIONAL Company	35
(3-4)	3D model for abrasive particle and workpiece (Isometric)	36
(3-5)	3D model for abrasive particle and workpiece (Side view)	36
(3-6)	the main interface for Ansys Explicit Dynamics	38
(3-7)	Engineering Data for Material Selection	38
(3-8)	importing the 3D model	39
(3-9)	Assigning Material for parts (1)	39
(3-10)	Assigning Material for parts (2)	39
(3-11)	determine meshing size	40
(3-12)	Setting Initial Condition for experiment	40
(3-13)	Setting Initial Velocity for Abrasive particle and vector component	40
(3-14)	Setting experiment duration and cycles	41
(3-15)	Determining pressure value	41
(4-1)	Plastic strain after particle impact to the target at Impact angle (30^o ,60^o ,90^o) at water Pressure 400 MPa	43
(4-2)	Plastic strain after particle impact to the target at impact angle (30^o ,60^o ,90^o) at water Pressure 400 MPa	44

(4-3)	Crater circularity definition (D1≡Minor carter diameter), (D2≡Major carter diameter) (C≡ Carter Geometry circularity).	45
(4-4)	Simulated craters circularity as a function of particle velocity and its impact angle at Pressure 400 MPa	46
(4-5)	Simulated craters circularity as a function of particle velocity and its impact angle at Pressure 600 MPa	47
(4-6)	Comparison of circularity between 400 MPa and 600 MPa	47

List of Tables

Table Number	Table Title	Page Number
(2-1)	Comparison of FEA simulations experimental results.	25
(3-1)	AINNOVATIVE INTERNATIONAL LTD Company AWJM Specifications	35
(3-2)	Abrasive Particles Properties	37
(3-3)	Workpiece Properties - Stainless Steel 1.4301 (AISI 304)	37
(3-4)	AWJM Parameters Assumptions for FEA Simulation	38
(4-1)	Minor carter diameter D_1, Major carter diameter D_2 and circularity C at water Pressure 400 MPa	45
(4-2)	Minor carter diameter D_1, Major carter diameter D_2 and circularity C at water Pressure 600 MPa	46

CHAPTER I

INTRODUCTION

CHAPTER I

INTRODUCTION

1.1 Preface

The insisting and continuous need to improve productivity and increasing level of Quality of products, furthermore some products complexity and requires of high precision, in addition to reduction in cost of production which led to rise up in performance of Manufacturing Processes.

Abrasive Water Jet Machining (AWJM) is considered to be a fast growing nonconventional technology that is capable of processing any material regardless of its properties with high Precision. Modern Water Jet Machining systems make use of high-pressure water jets (4,000 bar) forced through a tiny orifice (0.1–0.3 mm) which can generate huge cutting force.

1.2 Problem Statement

In this Research Simulation model will be designed to Study Influence of AWJM's parameters on the Process to Optimize the Abrasive Water Jet cutting process.

1.3 Research Importance

One of the most and critical drawbacks of AWJM is that it has low MRR, therefor this Research could help increasing Abrasive Waterjet Machine performance which will help to increase machine productivity.

1.4 Research Objectives

The ultimate objective is to Provide data that could help improving Abrasive Water jet cutting process performance.

- Main Objective is Optimization of Abrasive Water Jet Machine (**AWJM)** Cutting Process through simulation using Finite Element Method (**FEM).**
- Specific Objective is Studding **AWJM**'s Parameters (Impact Angle **α,** Water Pressure **P** and Traverse Rate **T**) influence on **AWJM** Cutting Process.

1.5 Scope of Research

Research falls within the field of production engineering, manufacturing, cutting Processes and operating material removal using Advanced machining processes

CHAPTER

II

LITERATURE REVIEW

CHAPTER II

LITERATURE REVIEW

2.1 Preface

The research take place in Non-Conventional machining or advanced machining Field Beside Finite Element Analysis (FEA) Field.

2.2 Advanced Machining Processes

The continuous and growing needs for accuracy, precision high quality beside mass production lead to revolution in manufacturing methods specifically Advanced machining processes which is considered as a great leap in manufacturing.

Nontraditional machining takes place when traditional machining processes are unsatisfactory or uneconomical:

- Workpiece material is too hard, strong, or tough.
- Workpiece is too flexible to resist cutting forces or too difficult to clamp.
- Part shape is very complex with internal or external profiles or small holes.
- Requirements for surface finish and tolerances are very high.
- Temperature rise or residual stresses are undesirable or unacceptable.

2.3 Advanced Machining Methods

2.3.1 Ultrasonic Machining (USM) principle

The Development of Ultrasonic Machining (**USM**) processes (see Figure 2.1) was instigated primarily by extensive use of hard, brittle materials and the need to machine them effectively (see Figure 2.2). Among other difficult machining problems, it has solved, USM is being used successfully to machine carbides, stainless steel, ceramics, and glass. The ultrasonic machining processes are performed by a cutting tool which oscillates at high frequency, typically 20,000 CPM in abrasive slurry. The shape of the tool corresponds to the shape to produce in the Workpiece. The high-speed reciprocations of the tool drive the abrasive grains across a small gap (a few thousandths of an inch) against workpiece [1] .The impact of the abrasive is the energy principally responsible for material removal.

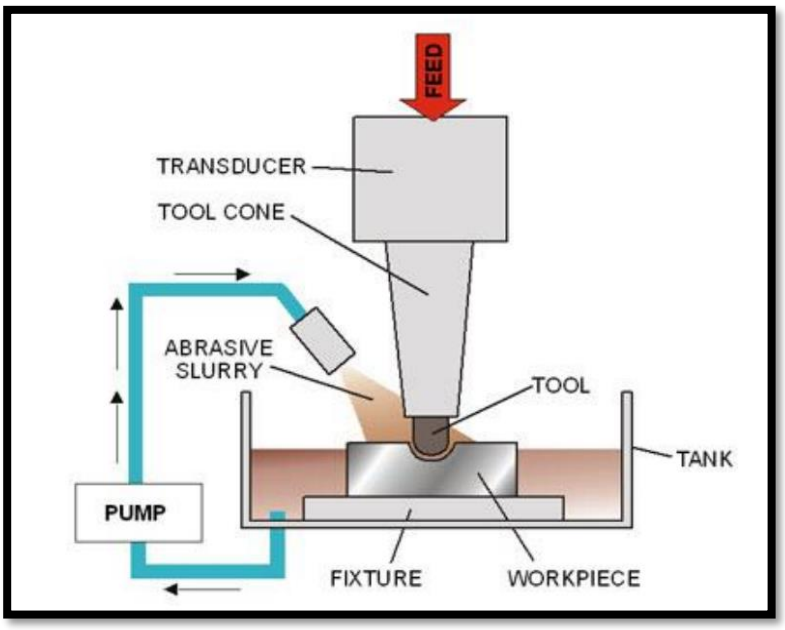

Figure (2.1) Ultrasonic Machining

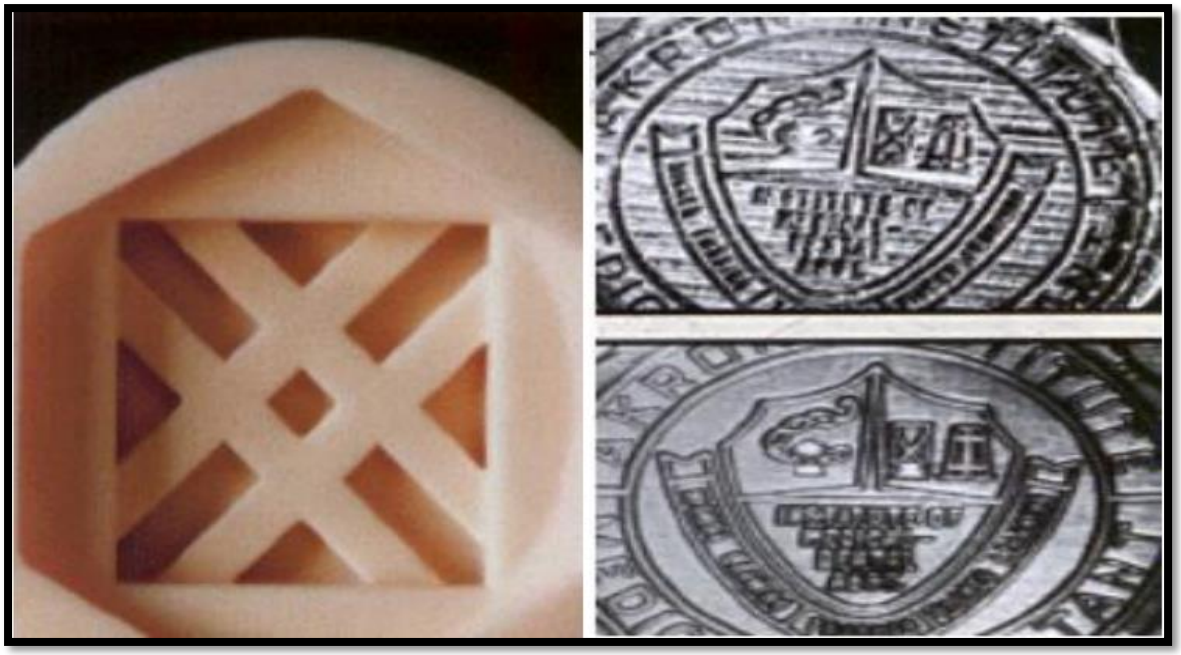

Figure (2.2) Finished Parts Processed Using USM

2.3.2 Laser beam machining (LBM)

Before discussing types of laser systems and their applications to machining, brief explanation of the fundamental principle of a laser must be shown at the atomic level an atom's orbital electrons can jump to higher energy levels (orbits further away from the nucleus) by absorbing quantum of simulating energy. When this occurs, the atom is said to be in the "excited" state and may then spontaneously emit, or radiate, the absorbed energy. Simultaneously, the electron drops back to its original orbit (ground state) or to an intermediate level. If another quantum of energy is absorbed by the electron while the atom is in the excited state, two quanta of energy are radiated, and the electron drops to its original level. This stimulated or radiated energy has precisely the same wavelength as that of the simulating energy. As a result, the simulating energy (pumping radiation) is amplified. In laser-beam machining (LBM), the source of energy is a laser (an acronym for light amplification by

stimulated emission of radiation), which focuses optical energy on the surface of the workpiece (see Figure 2.3). The highly focused, high-density energy source melts and evaporates portions of the workpiece in a controlled manner. This process (which does not require a vacuum) is used to machine a variety of metallic and nonmetallic materials. [1].

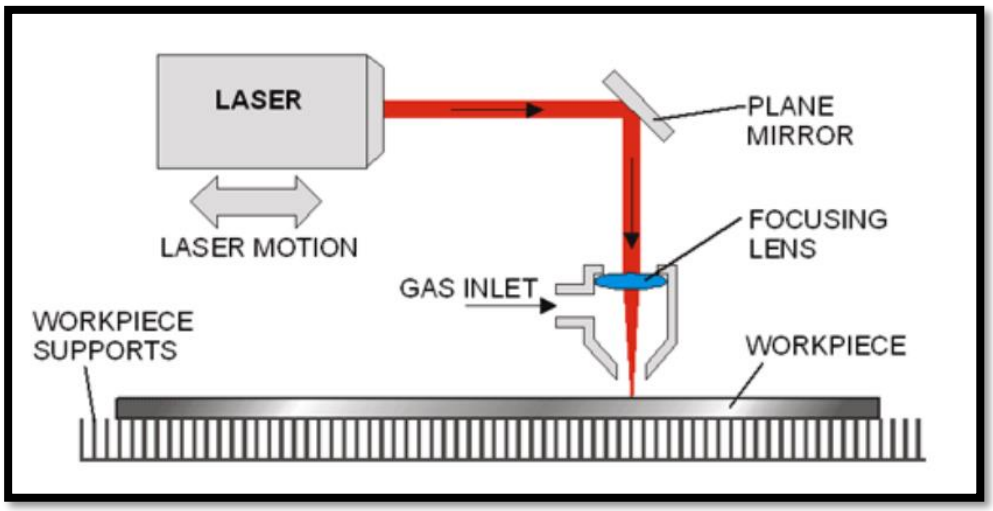

Figure (2.3) Laser beam machining

2.3.3 Electrical Discharge Machining (EDM)

Electrical Discharge Machining is the process of machining (see Figure 2.4) materials which sparks the area where the sparking takes place surrounded by dielectric material. The cutting tool called an electrode, does not physically contact the part being machined instead the electrode remains the distance of the spark away from the Workpiece. Thermal energy of the spark is used to machine the Workpiece. Only electrically conductive materials can be machined by EDM. Electrode material must also be electrically conductive. Dielectrics used in EDM are usually fluids, most commonly hydrocarbon oils [1].

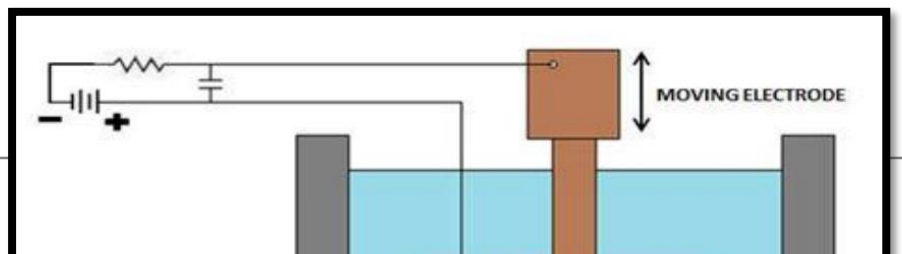

Figure (2.4) Electrical Discharge Machining (EDM)

2.3.4 Electrical Discharge Wire Machining (EDWM)

EDWM like EDM uses the thermal energy of spark to remove Workpiece material (see Figure 2.5). The spark melts a localized minute area of the part which is then flushed away.

Both the Workpiece and the wire are constantly flushed with a dielectric fluid at the area being machined. The dielectric deionized water or oil serves as a conductor for the current as well as coolant and means of removing the machine metal particles.

Electrode wire may be made of Brass, Copper, Tungsten, or molybdenum. The diameter of the wire may be varying from 0.003 to 0.012 inch (0.08 to 0.30 mm) [1].

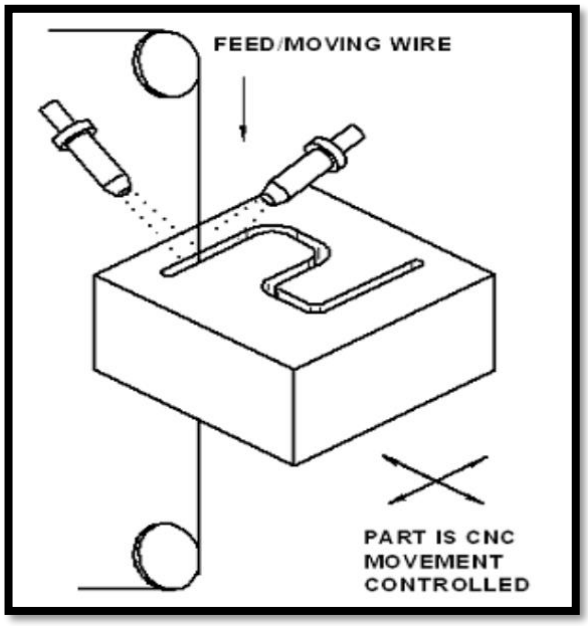

Figure (2.5) EDM wire machining

2.3.5 Chemical Machining (CM)

Chemical machining, basically an etching process, is the oldest nontraditional machining process (see Figure 2.6). Material is removed from a surface by chemical dissolution using chemical reagents, or etchants, such as acids and alkaline solution.

The Workpiece is immersed in a bath containing an etchant. The areas that are not required to be etched are masked with “cut and peel” tapes, paints, or polymeric materials. In chemical milling, shallow cavities are produced on plates, sheets, forgings, and extrusions for overall reduction of weight. Depths of removal can be as much as 12mm [1].

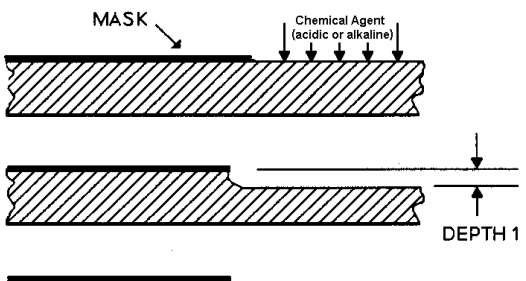

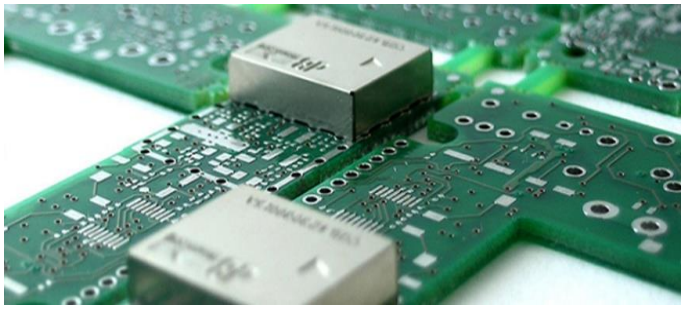

Figure (2.6) Chemical Machining

2.3.6 Electrochemical Machining (ECM)

Electrochemical machining (ECM) is basically the reverse of electroplating (see Figure 2.7). An electrolyte acts as current carrier, and the high rate of electrolyte movement in the Tool-Workpiece gap (typically 0.1 to 0.6 mm) washes metal ions away from the Workpiece (anode) before they have a chance to plate onto the tool (cathode). Note that the cavity produced is the female mating image of the tool shape [1].

The shaped tool either a solid or tubular form, is generally made of brass, copper, bronze, or stainless steel. The electrolyte is a highly conductive inorganic fluid, such as an aqueous solution of sodium nitrate. It is pumped through the passages in the tool at rates of 10 to 16 m/s. A DC power supply in the range from 10 to 25 V maintains current densities, which, for most applications, are 20 to 200 A/cm^2 of active machined surface.

The material-removal rate (MRR) in electrochemical machining for a current efficiency of 100% may be estimated from the equation

$$\mathbf{MRR} = \mathbf{CI} \qquad [1]$$

where MRR is in mm^3/min, **I** is the current in amperes, and **C** is a material constant, in mm3/A-min. For pure metals, **C** depends on the valence: The higher the valence, the lower is its value of C. Machines having current capacities as high as 40,000 A and as low as 5 A are available. The penetration rate of the tool is proportional to the current density. The material removal rate typically ranges between 1.5 and 4 mm3 per A-min. Because the metal-removal rate is a function only of the ion exchange rate, it is not affected by the strength, hardness, or toughness of the Workpiece.

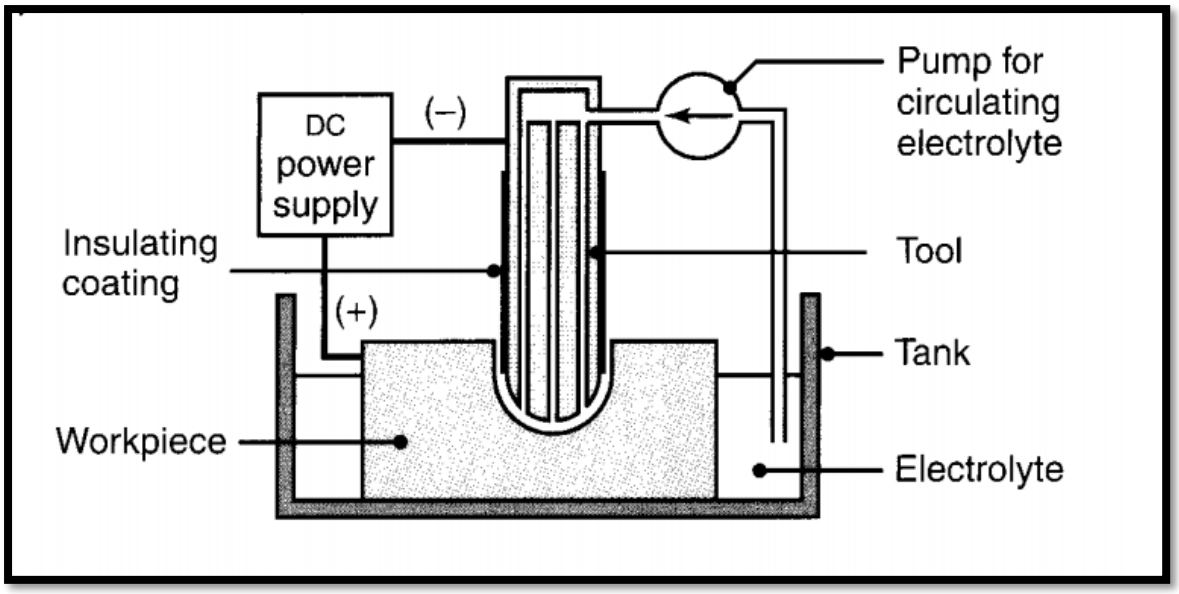

Figure (2.7) Electrochemical Machining (ECM)

2.3.7 Waterjet Machining

The water jet acts like a saw and cuts a narrow groove in the material. A pressure level of about 400 MPa is generally used for efficient operation,

Jet-nozzle diameters range between 0.05 and 1 mm. A water-jet cutting machine and its operation are shown in (see Figure 2.8). A variety of materials can be cut, including plastics, fabrics, rubber, wood products, paper, leather, insulating materials, brick, and composite materials with recent advances in control and motion technology.

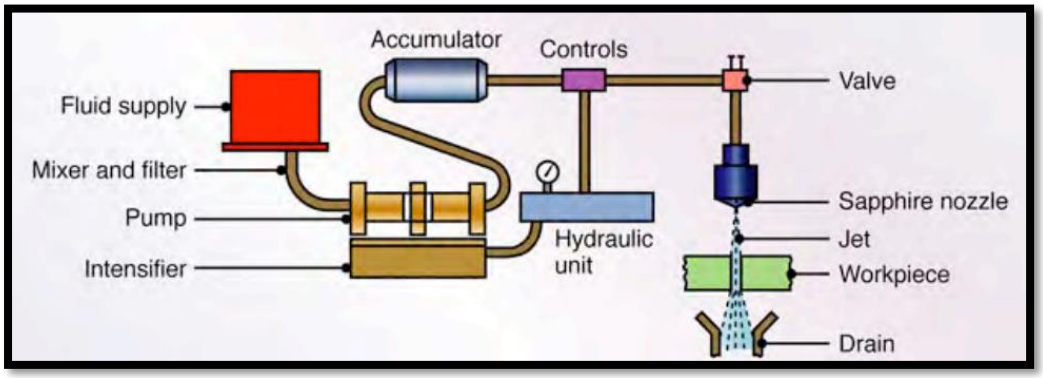

Figure (2.8) Waterjet Machining WJM

5-axes water jet machine cutting has become a reality (see Figure 2.9). Where the normal axes on a water jet are named X (back/forth), Y (left/right) and Z(up/down), a 5-axes system will typically add an axis (angle from perpendicular) and C axes (rotation around the Z-axis). Depending on the cutting head, the maximum cutting angle for the A axis can be anywhere from 55, 60, or in some cases even 90 degrees from vertical. As such, 5-axis cutting opens up a wide range of applications that can be machined on a water jet cutting machine [1].

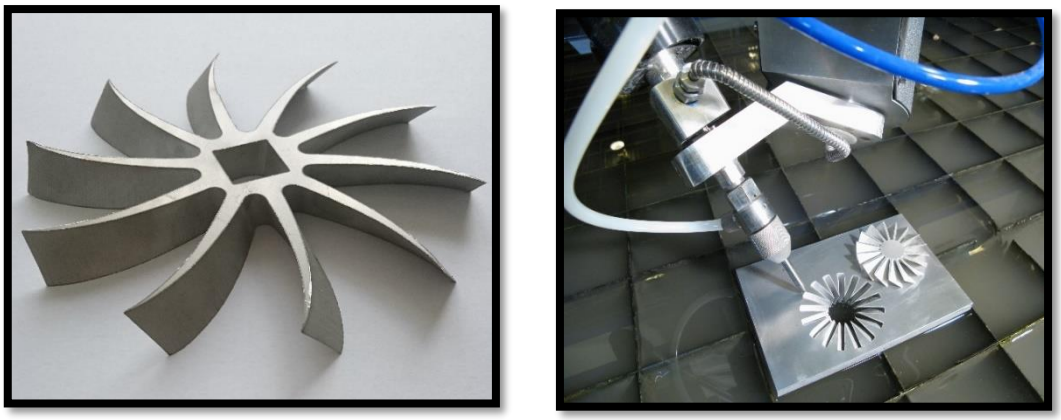

Figure (2.9) Finished parts with Waterjet Machining 5 axis

2.4 Abrasive Waterjet Machining (AWJM)

In abrasive-jet machining (AJM) (see Figure 2.11), a high-velocity jet of dry air, nitrogen, or carbon dioxide containing abrasive particles is aimed at the Workpiece surface under con-trolled conditions. The impact of the particles develops a sufficiently concentrated force to perform operations such as (a) cutting small holes, slots, or intricate patterns in very hard or brittle metallic and nonmetallic materials, (b) deburring or removing small flash from parts, (C) trimming and beveling, (d) removing oxides and other surface films, and (e) generally cleaning components with irregular surfaces [1].

The gas-supply pressure is on the order of 850 KPa, and the abrasive-jet velocity can be as high as 300 m/s and is controlled by a valve (see Figure 2.10). The nozzles are usually made of tungsten carbide or sapphire, both of which have abrasive Wear resistance [2].

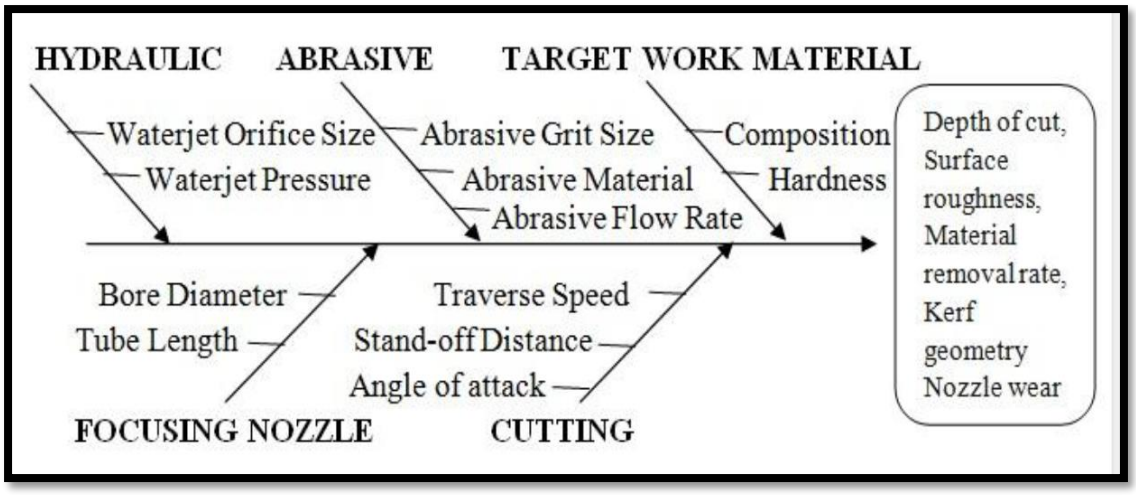

Figure (2.10) Process parameters influencing the AWJ cutting process

The abrasive size is in the range from 10 to 50 um. Because the flow of the free abrasives tends to round off corners, designs for abrasive-jet machining should avoid sharp corners. Also, holes made in metal parts tend to be tapered. There is some hazard involved in using this process, because of airborne particulates. The problem can be avoided by using the abrasive Water-jet machining process.

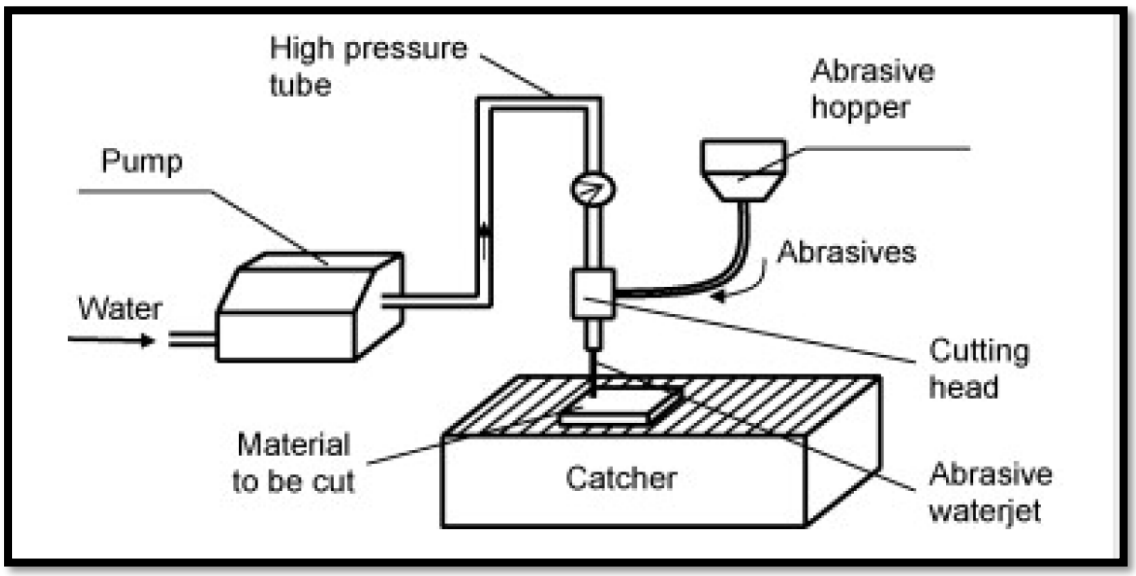

Figure (2.11) Abrasive Water Jet Machine AWJM

2.4.1 Previous Studies

A.A. Khan and M.M. Hague [3] analyses the performance of different abrasive particles in abrasive water jet machining of glass. They compare the effect of different abrasives on taper of cut by varying the stand-off distance, work feed rate, pressure. Garnet abrasive produce the largest taper of cut, followed by aluminum oxide, and silicon carbide. The study also describes that the taper of cut increases with increase in the stand-off distances because water jet gets widen with increase in stand-off distance. The taper of cut decreases with increase in jet pressure, with increase in pressure the cutting energy of jet increases. The depth of penetration of jet increases with increases in hardness of abrasives. M.A. Amir, A.K. Ahsan [4] conducted a practical study for analyzing the surface roughness and kerf taper ratio of glass/epoxy composite laminate machined using abrasive water jet machine. The various process parameters considered are abrasive types (2-level), hydraulic pressure (3-level), standoff distance (3-level), abrasive flow rate (3-level), traverse rate (3-level), cutting orientation (3-level). The optimization of AWJM was done with the use of Taguchi method and ANOVA (analysis of variance). The ratio of top kerf width to bottom kerf width is called Kerf taper ratio. Types of abrasives and traverse speed are insignificant parameter for surface roughness while hydraulic pressure is most significant factor that influences surface roughness in AWJM. Standoff distance (SOD), cutting orientation and abrasive mass flow rate are equally significant factors that influence surface roughness, but the kerf taper ratios are? influenced by hydraulic pressure, abrasive mass flow rate and cutting orientation. Abrasives type, standoff distance and traverse speed are most significant factors that had significant influences on kerf taper ratio. The quality of cutting in AWJM can be increased by increasing the kinetic energy of the

water jet. Ahmet Hascalilk, Ulas Aydas, Hakan Gurun [5] has carried out the study of effect of traverse speed on AWJM of Titanium alloy. The width of cutting, changes with changes in traverse speed. International Journal of Recent advances in Mechanical Engineering (IJMECH) Vol.3, No.3, August 2014 The study also reveals that the kerf taper ratio and surface roughness increases with increases in traverse speed. The increase in traverse speed reduces the interaction of abrasives particles and the work piece thus narrow kerf widths with a greater kerf taper ratio can be cut with AWJM.

J. John Rozario Jegaraj, N. Ramesh Babu [6] worked on 6063-T6 Aluminum alloy to find efficient strategy and quality cutting of materials with abrasive water jets considering the variation in orifice and focusing nozzle diameter in cutting. The study found that the effect of orifice size and focusing nozzle diameter on depth of cut, material removal rate, cutting efficiency, kerf geometry and surface roughness. The study suggested that a ratio of 3:1 between focusing nozzle diameter to orifice size was best suited combination to achieve the maximum depth of cut out of several combinations of focusing nozzle to orifice size. They suggest that the ratio of 5:1 and beyond cause ineffective entrainment of abrasives in cutting head. The investigation also analyzes that the increase in hydraulic pressure for different combinations of orifice and focusing nozzle size the depth of cut increases. The material removal rate also increases with an increase in the size of focusing nozzle up to 1.2 mm diameter and further increase tends to decrease the material removal rate. The abrasive flow rate has less significant on kerf width. This study suggests that taper of kerf can be minimized by maintaining the orifice size and focusing nozzle size within certain limits ranging from 0.25–0.3 mm and 1.2 mm, respectively. The surface quality does not depend on the increase in the size of orifice

and focusing nozzle but larger size of orifice, produce better surface finish on cut surface.

J. Wang, W.C.K. Wong [7] conducted a statistically designed experiment to study the effect of abrasive water jet cutting of metallic coated sheet steels. The relationship between kerf characteristics and process parameters are also investigated in this experiment. An empirical model was developed for kerf geometry and quality of cut for the prediction and optimization of AWJ cutting performance. A three-level four-factor full factorial designed experiment performed for analyzing the AWJM process. The various process parameters used are water jet pressure, traverse speed, abrasive flow rate and standoff distance (SOD). The study found that the top and bottom kerf widths increase with increase in hydraulic pressure, standoff distance but the rate of increase for the bottom kerf width is smaller. The traverse speed produces an inverse effect on the top kerf width and bottom kerf widths but at same time the kerf taper increase as the traverse speed increase. The surface roughness of the cut surface decreases with an increase in the abrasive flow rate.

Mohemed Hashish [8] observed that as the pressure increases the power required for cutting get reduced drastically. This suggests that cutting at higher pressure is more efficient than at low pressure for the same power consumption. Plain waterjets are capable of cutting the sheet metals at pressure of 600 Mpa. Elevated pressure promise cost reduction due to reduction in abrasive usage or increased cutting speed. The study shows that the depth of cut increases with increases in water pressure.

H. Hocheng and K.R. Chang [9] conducted experimental evaluation on the kerf formation over ceramic plate cut with an abrasive water jet. It found that a critical combination of hydraulic pressure, abrasive flow rate and traverse speed are required for through- out cut of ceramics, below

which it cannot be achieved for certain thickness. A sufficient supply of hydraulic energy, fine mesh abrasives at moderate speed gives smooth kerf surface. By experiment investigation they found that the kerf width increases with increasing these factors such as pressure, traverse speed, abrasive flow rate and abrasive size. They also found that the taper ratio increases with increase in traverse speed and decreases with increase pressure and abrasive size. Abrasive flow rate has no influence over taper ratio.

Mahabalesh Palleda [10] investigated the influence of the different chemical such as acetone, phosphoric acid and polymer (polyacrylamide) in the ratio of 30% chemicals with 70% of water. He also analyzes the effect of standoff distance on the taper angles and material removal rates (MRR) of drilled holes in the abrasive water jet machining process. It found that the Material removal increases with slurry added with polymers compare to the other three slurries. The study also reveals that the MRR increase with increase of standoff distance, because momentum of impacting abrasive particles on the work surface creating craters of more depth. As the standoff distance increase the taper holes of drilled holes' decreases. The use of phosphoric acid combination and the slurry with acetone combination with slurry observes less taper in drilled holes than with the plain water slurry. Taper in drilled holes are almost nill by using polymer additives. The study also found that the material removal rate increases with increase in chemical concentration of acetone and phosphoric acid in the slurry up to a certain limit and then decreases. In case of polymer with the slurry the material removal is found to increases continuously.

Alberdi, A. Suarez, T. Artaza, G.A. Escobar-Palafox, K. Ridgway, [11] studied the behavior of a machinability model in composite materials. The machinability index of different composite materials is very different, so they have to be studied separately. The machinability index may be related to the tensile modulus and/or to the fiber content of the composite materials, but still now there is no solid evidence to relate machinability index with the material property and researches are required to relate the machinability index with the material properties. The separation speed has to be re-defined for this kind of material as the traverse rate at which the material can be cut without delamination. C. Ma, R. T. Deam [12] studied the kerf geometry of cut in abrasive waterjet machining using an optical microscope. The kerf width developed on the work has shown that there are two regions, called the developing stage and the fully developed stage. The first region is the developing stage, and it ends after about 2 mm of the cutting depth. The developing stage is due to the velocity profile of the jet changing from a uniform profile to a fully developed flow in a groove. The velocity profile developed is similar to the velocity profile developed when flow enters a pipe from a large tank.

In the second section, the fully developed stage which starts from 2 mm to the cutting depth and the cutting width varies with depth, depending on the cutting speed. The kerf width increases with low cutting speed and narrows down at high cutting speeds.

M. Chithirai Pon Selvan, Dr. N. Mohana Sundara Raju, Dr. R. Rajavel [12] had investigated the effects of process parameters on the depth of cut in abrasive waterjet machining of cast iron.

They investigated that the depth of cut increases with increases in water pressure, when mass flow rate, standoff distance, traverse speed was kept constant. Increases in abrasive flow rate also increase the depth of cut

keeping other parameters constant. The depth of cut is found to decrease with increase in traverse speed because the contact of abrasive particle over the Workpiece is for shorter duration. It is also found that the depth of cut decreases with increase in the standoff distance between nozzle and work piece keeping other operational parameters constant.

In 2006 paper presented by [M. Junkara, B. Jurisevica, *, M. Fajdigab, M. Grahc] under title [Finite element analysis of single-particle impact in abrasive water jet machining] [20] to compare between Experimental and simulation data that given by ANSYS Software for [single-particle impact in abrasive water jet machining with different angles and velocities, and comparison showed very good agreement [see Appendices].

2.5 Finite Element Analysis (FEA)

FEA becomes the best mean to show how a product reacts to real-world forces, vibration, heat, fluid flow, and other physical effects. Finite element analysis shows whether a product will break, wear out, or work the way it was designed. It is called analysis, but in the product development process, it is used to predict what is going to happen when the product is used.

FEA works by breaking down a real object into a large number (thousands to hundreds of thousands) of finite elements, such as little cubes. Mathematical equations help predict the behavior of each element. A computer then adds up all the individual behaviors to predict the behavior of the actual object [13].

The process of representing a physical domain with finite elements is referred to as meshing, and the resulting set of elements is known as the finite element mesh.

As most of the commonly used element geometries have straight sides, it is generally impossible to include the entire physical domain in the element mesh if the domain includes curved boundaries. Such a situation is shown in (Figure 2.12-a), where a curved-boundary domain is meshed (quite coarsely) using square elements. A refined mesh for the same domain is shown in (Figure 2.12-b), using smaller, more numerous elements of the same type. Note that the refined mesh includes significantly more of the physical domain in the finite element representation and the curved boundaries are more closely approximated. (Triangular elements could approximate the boundaries even better.)

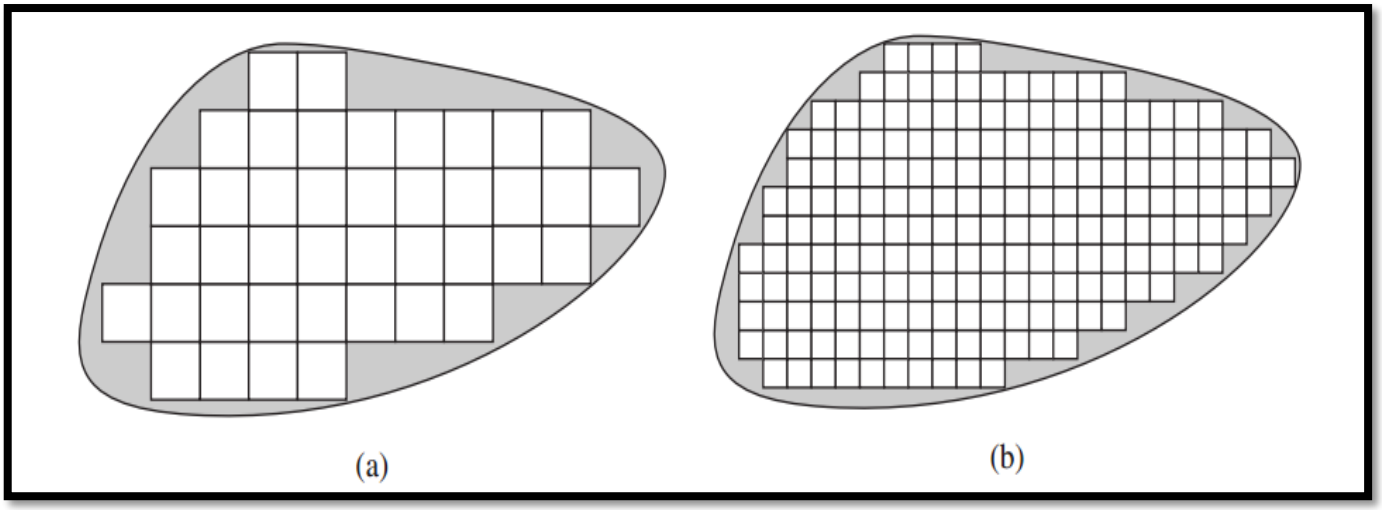

Figure (2-12) curved-boundary mesh

(Figure 2.12-a) Arbitrary curved-boundary domain modeled using square elements. Stippled areas are not included in the model. A total of 41 elements is shown. (Figure 2.12-b) Refined finite element mesh showing reduction of the area not included in the model. A total of 192 elements is shown.

If the interpolation functions satisfy certain mathematical requirements, a finite element solution for a particular problem converges to the exact solution of the problem. That is, as the number of elements is increased and the physical dimensions of the elements are decreased, the finite element solution changes incrementally. The incremental changes decrease with the mesh refinement process and approach the exact solution asymptotically. To illustrate convergence, we consider a relatively simple problem that has a known solution. (see Figure 2.13), depicts a tapered, solid cylinder fixed at one end and subjected to a tensile load at the other end. Assuming the displacement at the point of load application to be of interest, a first approximation is obtained by considering the cylinder to be uniform, having a cross-sectional area equal to the average area of the cylinder (Figure 2.13-b) The uniform bar is a link or bar finite element [14], so our first approximation is a one-element, finite element model.

The solution is obtained using the strength of materials theory. Next, we model the tapered cylinder as two uniform bars in series, as in (Figure 2.13-c). In the two-element model, each element is of length equal to half the total length of the cylinder and has a cross-sectional area equal to the average area of the corresponding half-length of the cylinder. The mesh refinement is continued using a four-element model, as in (Figure 2.12-d), and so on. For this simple problem, the displacement of the end of the cylinder for each of the finite element models is as shown in (Figure 2.13),

where the dashed line represents the known solution. Convergence of the finite element solutions to the exact solution is clearly indicated [15].

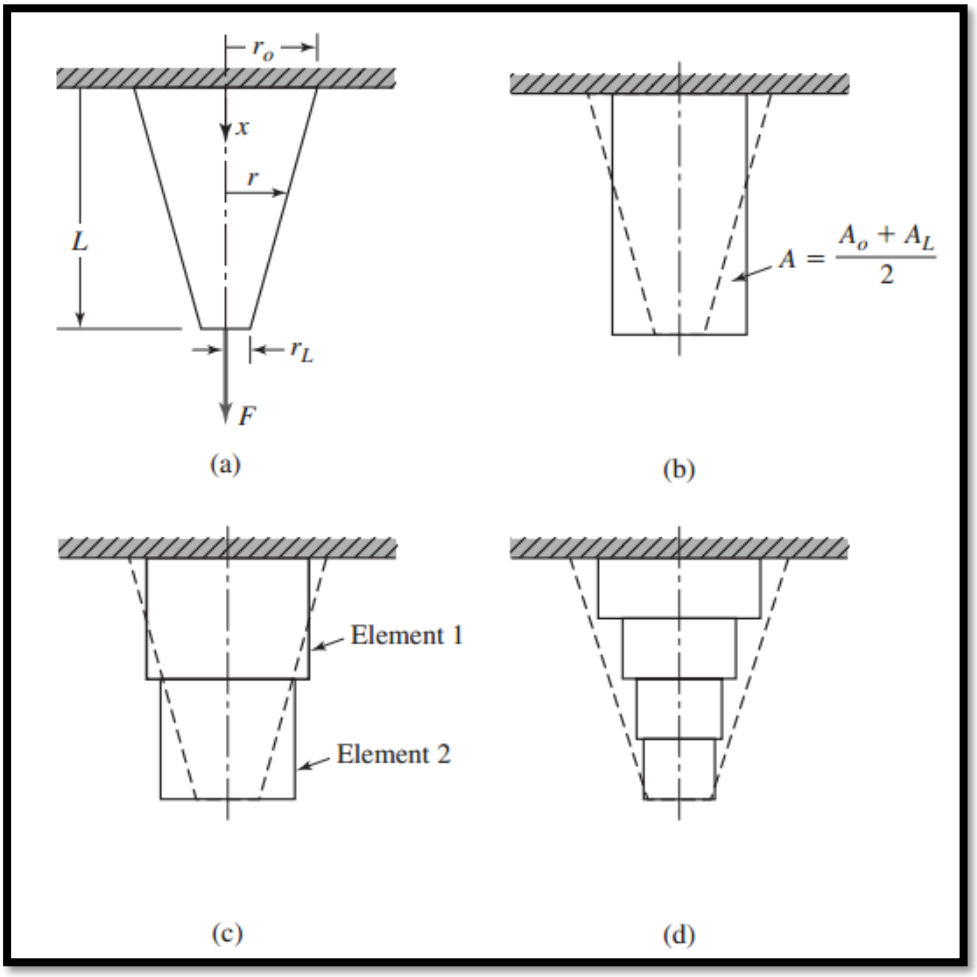

Figure 2-13: Tapered circular cylinder subjected to tensile loading

Where r_0 is base radius of the Tapered circular cylinder, r_L is top radius of the Tapered circular cylinder, L is the length of Tapered circular cylinder, F is the subjected force, A is the mean Cross Section Area of Tapered circular cylinder, When A_0 and A_L is the base and top Cross Sectional Areas for the Tapered circular cylinder.

(Figure 2.13-a) Tapered circular cylinder subjected to tensile loading: $r(x) = r_0 - (x/L)(r_0 - r_L)$, (Figure 2.13-b) Tapered cylinder as a single axial (bar) element using an average area. Actual tapered cylinder is shown as

dashed lines. (Figure 2.13-c) Tapered cylinder modeled as two, equal-length, finite elements. The area of each element is average over the respective tapered cylinder length. (Figure 2.13-d) Tapered circular cylinder modeled as four, equal-length finite elements. The areas are average over the respective length of cylinder (element length =L/4).

CHAPTER

III

METHODOLOGY

CHAPTER III

METHODOLOGY

3.1 Preface

This chapter discuss Abrasive waterjet machine parts and 3D design addition to ANSYS simulation verification, simulation Model and Simulation Constrains.

3.2 SolidWorks Design Software

SolidWorks (stylized as SOLIDWORKS), is a solid modeling computer-aided design (CAD) and computer-aided engineering (CAE) software program that runs on Microsoft Windows. The SolidWorks is produced by the Dassault Systèmes— a subsidiary of Dassault Systèmes, S. A. based in Vélizy, France— since 1997.

SolidWorks is currently used by over 2 million engineers[2] and designers at more than 165,000 companies worldwide. In 2011–2012, the fiscal revenue for SolidWorks was reported $483 million. [18]

SolidWorks is a solid modeler, and utilizes a parametric feature-based approach to create models and assemblies. The software is written on PARASOLID-kernel.

Parameters refer to constraints whose values determine the shape or geometry of the model or assembly. Parameters can be either numeric parameters, such as line lengths or circle diameters, or geometric parameters, such as tangent, parallel, concentric, horizontal or vertical, etc. Numeric parameters can be associated with each other through the

use of relations, which allows them to capture design intent. Design intent is how the creator of the part wants it to respond to changes and updates. For example, you would want the hole at the top of a beverage can to stay at the top surface, regardless of the height or size of the can. SolidWorks allows the user to specify that the hole is a feature on the top surface, and will then honor their design intent no matter what height they later assign to the can.

Features refer to the building blocks of the part. They are the shapes and operations that construct the part. Shape-based features typically begin with a 2D or 3D sketch of shapes such as bosses, holes, slots, etc. This shape is then extruded or cut to add or remove material from the part. Operation-based features are not sketch-based, and include features such as fillets, chamfers, shells, applying draft to the faces of a part, etc. screen shot captured from a SolidWorks top-down design approach.

Building a model in SolidWorks usually starts with a 2D sketch (although 3D sketches are available for power users). The sketch consists of geometry such as points, lines, arcs, conics (except the hyperbola), and splines. Dimensions are added to the sketch to define the size and location of the geometry. Relations are used to define attributes such as tangency, parallelism, perpendicularity, and concentricity. The parametric nature of SolidWorks means that the dimensions and relations drive the geometry, not the other way around. The dimensions in the sketch can be controlled independently, or by relationships to other parameters inside or outside of the sketch.

In an assembly, the analog to sketch relations are mates. Just as sketch relations define conditions such as tangency, parallelism, and concentricity with respect to sketch geometry, assembly mates define equivalent relations with respect to the individual parts or components, allowing the easy construction of assemblies. SolidWorks also includes additional advanced mating features such as gear and cam follower mates, which allow modeled gear assemblies to accurately reproduce the rotational movement of an actual gear train [19].

Finally, drawings can be created either from parts or assemblies. Views are automatically generated from the solid model, and notes, dimensions and tolerances can then be easily added to the drawing as needed. The drawing module includes most paper sizes and standards (ANSI, ISO, DIN, GOST, JIS, BSI and SAC).

3.3 ANSYS Software

Ansys, Inc. is an American Computer-aided engineering software developer headquartered south of Pittsburgh in Cecil Township, Pennsylvania, United States. Ansys publishes engineering analysis software across a range of disciplines including finite element analysis, structural analysis, computational fluid dynamics, Explicit and implicit methods, and heat transfer.

3.3.1 History

The company was founded in 1970. by John A. Swanson as Swanson Analysis Systems, Inc. (SASI). Its primary purpose was to develop and market finite element analysis software for structural physics that could simulate static (stationary), dynamic (moving) and thermal (heat transfer)

problems. SASI developed its business in parallel with the growth in computer technology and engineering needs. The company grew by 10 percent to 20 percent each year, and in 1994 it was sold to TA Associates. The new owners took SASI's leading software, called ANSYS, as their flagship product and designated ANSYS, Inc. as the new company [16].

3.3.2 ANSYS Advantages

A. Unequalled Depth

The ANSYS commitment is to provide unequalled technical depth in any simulation domain. Whether it's structural analysis, fluids, thermal, electromagnetics, meshing, or process & data management we have the level of functionality appropriate for your requirements. Through both significant R&D investment and key acquisitions, the richness of our technical offering has flourished. We offer consistent technology solutions, scalable from the casual user to the experienced analyst, and seamless in their connectivity. In addition, we have world class expertise for all of these domains, available to help you implement your ANSYS technology successfully [17].

B. Unparalleled Breadth

Unlike other engineering simulation companies, who may possess competence in one, or maybe two, fields, ANSYS can provide this richness of functionality across a broad range of disciplines, whether it be explicit, structural, fluids, thermal, or electromagnetics. All of these domains are supported by a complete set of analysis types and wrapped by a unified set of meshing tools. Together, these domains form the cornerstones of the ANSYS portfolio for Simulation Driven Product Development, and constitute a complete portfolio of unparalleled breadth in the industry [17].

C. Comprehensive Multiphysics

A strong foundation for Multiphysics sets ANSYS apart from other engineering simulation companies. Our technical depth and breadth, in conjunction with the scalability of our product portfolio, allows us to truly couple multiple physics in a single simulation. Technical depth in all fields is essential to understand the complex interactions of different physics. The portfolio breadth eliminates the need for clunky interfaces between disparate applications. The ANSYS capability in Multiphysics is unique in the industry; flexible, robust and architected in ANSYS Workbench to enable you to solve the most complex coupled physics analyses in a unified environment.

D. Engineered Scalability

Scalability is a critical consideration when considering software for both current and long term objectives. At ANSYS engineered scalability means flexibility you need has been designed for your particular needs. ANSYS provides you with the ability to apply the technology at a level that is appropriate for the size of the problem, execute it on a full range of computing resources, based on what's appropriate and available, and finally the ability to deploy the technology within your company's user community. The result is efficient usage and optimum return on your investment, whether you have a single user or an enterprise-wide commitment to Simulation Driven Product Development. As your requirements grow and the level of sophistication and maturity evolves, the technology from ANSYS also will scale up accordingly [17].

E. Adaptive Architecture

Adaptive software architectures are mandatory for today's world of engineering design and development where a multiplicity of different CAD, PLM, in-house codes and other point solutions typically comprise the overall design and development process. A software environment is

needed which anticipates these needs and gives you the tools and system services for customization as well as interoperability with other players. Such adaptability is a mandatory requirement and characteristic of the ANSYS simulation architecture, enabling your organization to apply the software in a manner which fits with your philosophy, environment and processes. ANSYS Workbench can be the backbone of your simulation strategy, or peer-to-peer with other software environments, or ANSYS technology can be a plug-in to your CAE supplier of choice. The ANSYS commitment to Simulation Driven Product Development is the same in any case [17].

3.3.3 Products

F. ANSYS Autodyn

ANSYS Autodyn is a computer simulation tool for simulating the response of materials to short duration severe loadings from impact, high pressure or explosions [16].

G. ANSYS CFD, CFX

ANSYS CFD, CFX, and related software are Computational Fluid Dynamics software tools used by engineers for design and analysis. These tools can simulate fluid flows in a virtual environment — for example, the fluid dynamics of ship hulls; gas turbine engines (including the compressors, combustion chamber, turbines and afterburners); aircraft aerodynamics; pumps, fans, HVAC systems, mixing vessels, hydro cyclones, vacuum cleaners, etc.

H. ANSYS HFSS

ANSYS HFSS is a Finite Element Analysis tool for simulating full-wave electromagnetic fields. HFSS incorporates finite element, integral

equation, and hybrid methods to solve a wide range of microwave, RF and high-speed digital applications.

I. ANSYS Maxwell

ANSYS Maxwell is a Finite Element Analysis tool for electromagnetic field simulation, primarily for engineers tasked with designing and analyzing electromagnetic and electromechanical devices, including motors, actuators, transformers, sensors and coils. ANSYS Maxwell incorporates finite element method solvers to solve static, frequency-domain, and time-varying electromagnetic and electric fields [16].

J. ANSYS Mechanical

ANSYS Mechanical software is a comprehensive FEA analysis (finite element) tool for structural analysis, including linear, nonlinear and dynamic studies. The engineering simulation product provides a complete set of elements behavior, material models and equation solvers for a wide range of mechanical design problems. In addition, ANSYS Mechanical offers thermal analysis and coupled-physics capabilities involving acoustic, piezoelectric, thermal–structural and thermo-electric analysis [18].

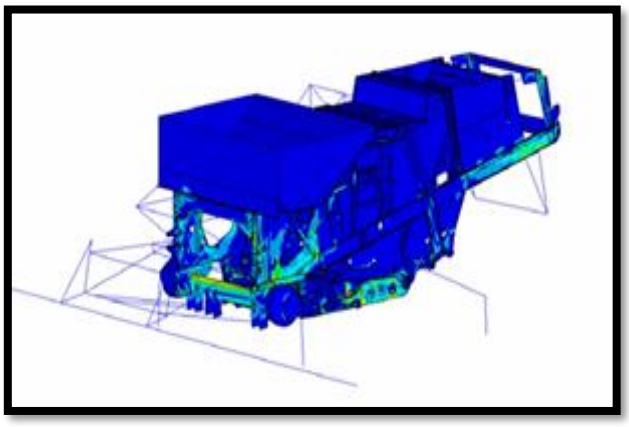

Figure (3-1) Vehicle Analysis using ANSYS Mechanical

3.3.4 Explicit Dynamics

The design of products that need to survive impacts or short-duration high-pressure loadings can be greatly improved with the use of ANSYS explicit dynamics solutions. These specialized problems require advanced analysis tools to accurately predict the effect of design considerations on product response to severe loadings. Understanding such complex phenomena is especially important when it is too expensive or impossible to perform physical testing.

The ANSYS explicit dynamics product suite helps you gain insight into the physics of short-duration events for products that undergo highly nonlinear, transient dynamic events. These specialized, accurate and easy-to-use tools have been designed to maximize productivity [19].

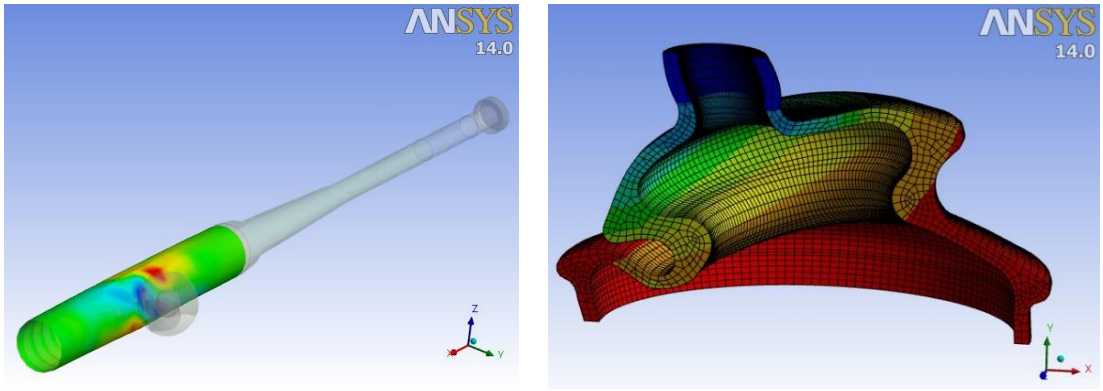

Figure (3-2) Products Analysis using ANSYS Explicit Dynamics

3.4 3D Model Design

3D Model Design built (see Figure 3-3) using **SOLIDWORKS** Designing Software according to Specification of Abrasive Water Jet Machine from **AINNOVATIVE INTERNATIONAL LTD** [21] as (see Table 3-1):

Table 3-1: AINNOVATIVE INTERNATIONAL LTD Company AWJM Specifications

Specification		
X Travel	1500	mm
Y Travel	2500	mm
Z Travel	150	mm
Maximum Load Capacity	250	kg/m2
Traverse Speed	5	m/min
Contour Speed	5	m/min
Linear Positioning Accuracy	0.1	mm
Linear Positioning Repeatability	0.05	mm
Power supply	380 ~ 415	V
	50	Hz
	AC 3 Phase	

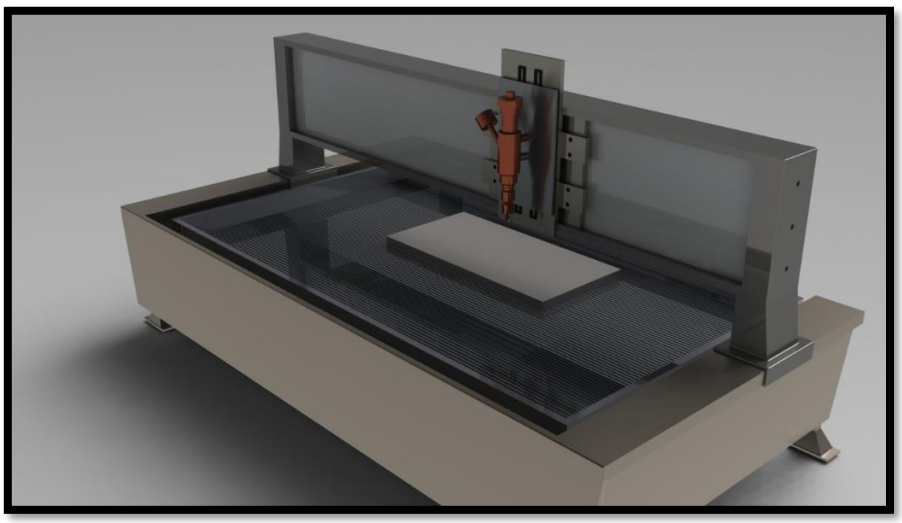

Figure (3-3): 3D Model for Abrasive water jet machine according to AINNOVATIVE INTERNATIONAL Company

3.5 Explicit Finite Element Analysis Simulation

Eighteen Experiments FEA simulation will be conducted to study the influence of impact Angle travers speed and operational pressure.

3.5.1 Simulation Model

3D Model Design was built using **SOLIDWORKS Designing Software** to represent Abrasive Particle and Workpiece (see Figure 3-4 and Figure 3-5).

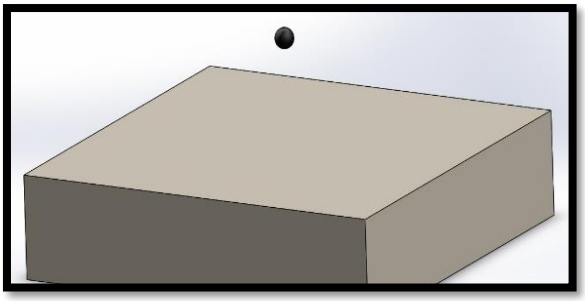

Figure (3-4): 3D model for abrasive particle and workpiece (Isometric)

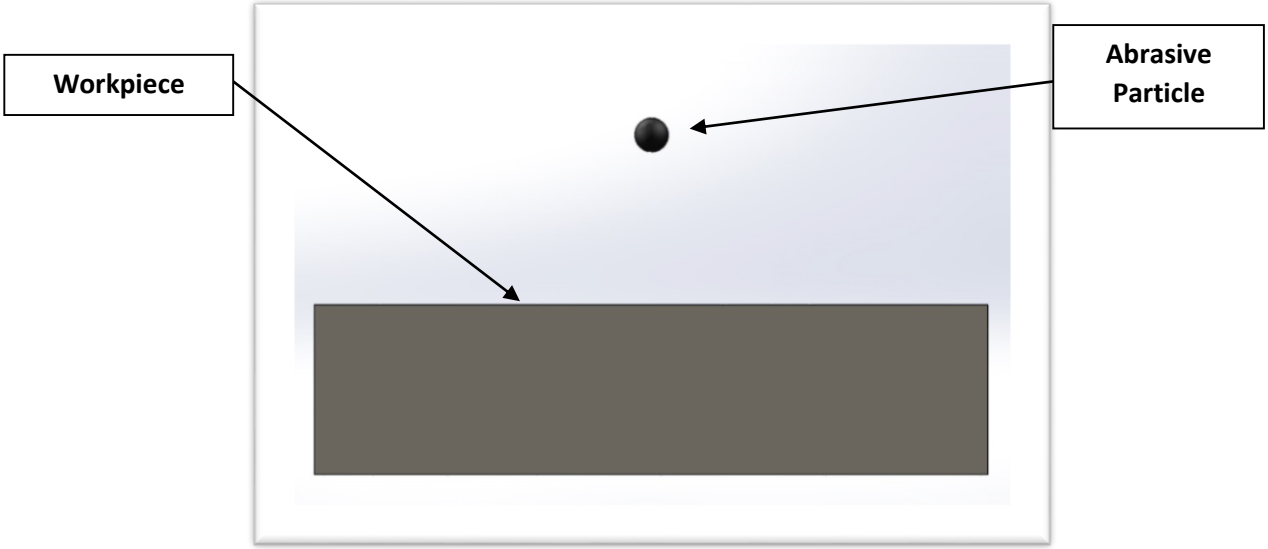

Figure (3-5): 3D model for abrasive particle and workpiece (Side view)

3.5.2 Simulation Constrains

Constrains were set to Simulate the real Life Conditions, material Properties for Abrasive Particle and Workpiece as described in (Table 3-2 & Table 3-3), also AWJM Parameters Assumptions for FEA Simulation had been described in (Table 3-4).

Table 3-2: Abrasive Particles Properties

Abrasive particles Properties – Al_2O_3		
Particles shape	Spherical	
Particles diameter	100	mm
Abrasive density	3900	kg/m3
Elasticity module	1×10^5	MPa
Yield module	8000	MPa
Gruneisen Coefficient	0.5	

Table 3-3: Workpiece Properties - Stainless Steel 1.4301 (AISI 304)

Workpiece Properties - Stainless Steel 1.4835		
Density	7860	kg/m3
Elasticity module	0.73×10^5	MPa
Yield Stress	316	MPa
Tensile Strength	623	MPa
Elongation	55%	
Gruneisen Coefficient	1.67	

Table 3-4: AWJM Parameters Assumptions for FEA Simulation

Impact Angle (Degree)	Water Pressure **P** = (400 MPa) Particle Velocity at The Impact **T** (m/s)			Water Pressure **P** = (600 MPa) Particle Velocity at The Impact **T** (m/s)		
α = 30 ^{O}	180	200	220	180	200	220
α = 60 ^{O}	180	200	220	180	200	220
α = 90 ^{O}	180	200	220	180	200	220

3.5.3 Simulation Procedure

1. After Opening Explicit Dynamics at ANSYS Software interface. all sub categories to conduct the simulation (Engineering Data, Geometry, Model, Setup, Solution, Result) (see Figure 3-6).

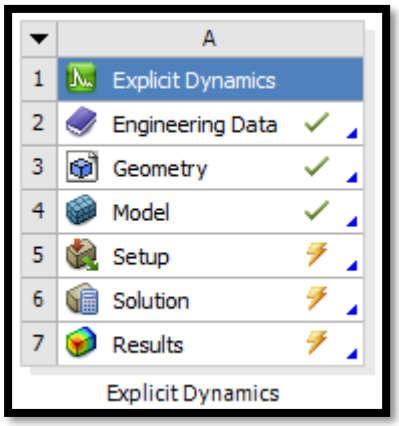

Figure (3-6): the main interface for Ansys Explicit Dynamics

2. From **Engineering Data** Tap materials that will be used in experiment selected from ANSYS Software Library or it can be created and described and be added to ANSYS Library (see Figure 3-7).

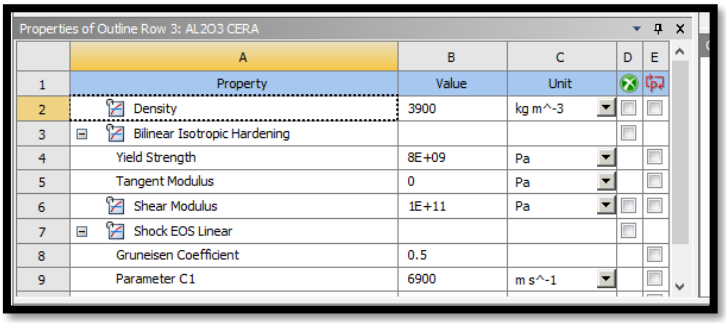

Figure (3-7): Engineering Data for Material Selection

3. From **Geometry** Tap 3D model imported, Ansys is integrated with many 3D design software and 3d extensions (see Figure 3-8), in this research 3D model for abrasive grain and workpiece with (. STEP) extension was exported from SOLIDWORKS Software.

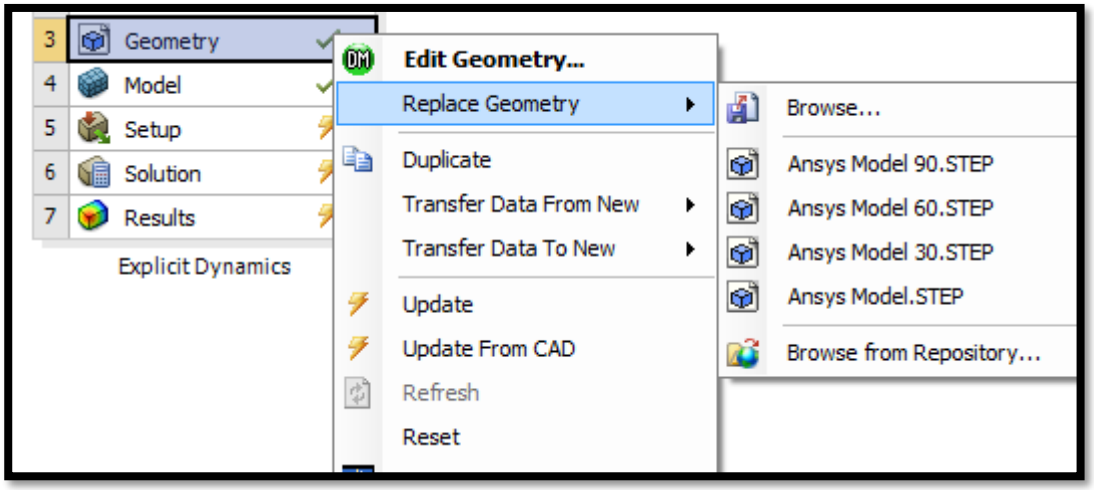

Figure (3-8): importing the 3D model

4. In **Model** Tap

A- Assigning Material for models (Al_2O_3) for abrasive grain particle and (Stainless Steel 1.4835) for workpiece (see Figure 3-9 & 3-10).

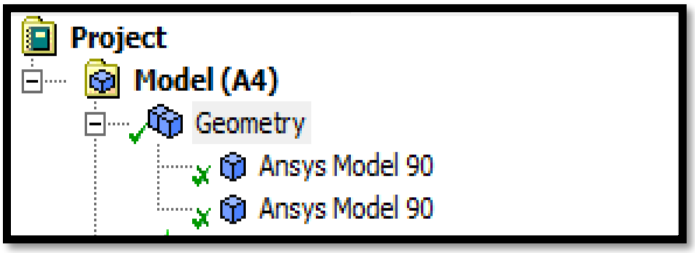

Figure (3-9): Assigning Material for parts (1)

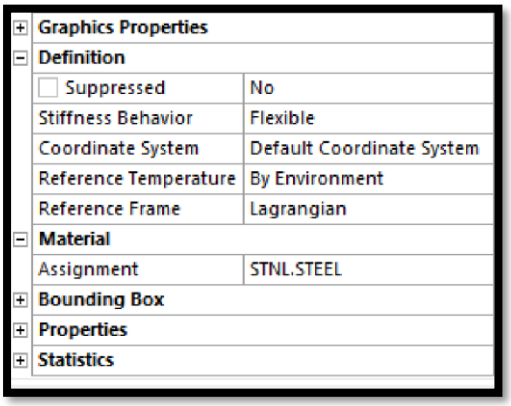

Figure (3-10): Assigning Material for parts (2)

B- Set sizing for mesh, smaller size division test accuracy increased but time duration will extend.in this research mesh size set to (5.5 µm) value (see Figure 3-11).

Defaults	
Physics Preference	Explicit
Relevance	0
Sizing	
Use Advanced Size Function	Off
Relevance Center	Fine
Element Size	5.5e-003 mm
Initial Size Seed	Active Assembly
Smoothing	High
Transition	Slow
Span Angle Center	Coarse
Minimum Edge Length	2.2159e-002 mm

Figure (3-11) determine meshing size

C- Initial Condition described, Initial Velocity described (see Figure 3-12), in case it was vertical or horizontal its define directly, in case it was diagonal Vector components calculated (see Figure 3-13).

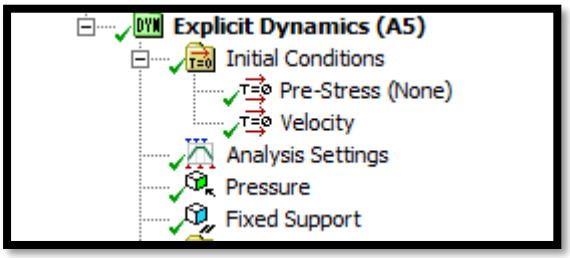

Figure (3-12): Setting Initial Condition for experiment

Scope	
Scoping Method	Geometry Selection
Geometry	1 Body
Definition	
Input Type	Velocity
Define By	Components
Coordinate System	Global Coordinate System
X Component	0. mm/s
Y Component	-2.2e+005 mm/s
Z Component	0. mm/s
Suppressed	No

Figure (3-13): Setting Initial Velocity for Abrasive particle and vector component

D- In Analysis settings cycles of experiment and duration of every cycle defined, in this experiment number of cycles set by 35000 cycles and duration is 0.000002(see Figure 3-14).

Analysis Settings Preference	
Type	Program Controlled
Step Controls	
Resume From Cycle	0
Maximum Number of Cycles	35000
End Time	2.e-006 s
Maximum Energy Error	0.1
Reference Energy Cycle	0
Initial Time Step	Program Controlled
Minimum Time Step	Program Controlled
Maximum Time Step	Program Controlled
Time Step Safety Factor	0.9

Figure (3-14): Setting experiment duration and cycles

E- Pressure on particle Determent by 400 MPa then it increased to be 600 MPa (see Figure 3-15).

Scope	
Scoping Method	Geometry Selection
Geometry	1 Face
Definition	
Type	Pressure
Define By	Normal To
Magnitude	400. MPa (step applied)
Suppressed	No

Figure (3-15): Determining pressure value

F- Fixed support defined the four around surface on workpiece.

5. Then in **Results** Tap solving methods Determent which is (Equivalent Plastic Strain) to show displacement and deformation.

CHAPTER IV

RESULTS AND RESULTS DISCUSSION

CHAPTER IV

RESULTS AND RESULTS DISCUSSION

4.1 FEA Simulation Results:

Eighteen experiments conducted, two deferent Water Pressures 400 MPa (see Figure 4-1) and 600 MPa (see Figure 4-2), three Impact angles 30^{o}, 60^{o} and 90^{o}, and three deferent Traverse Rates 180 m/s 200 m/s 220 m/s. every time all parameters fixed Except simulation subject parameter Results show Carter Geometry.

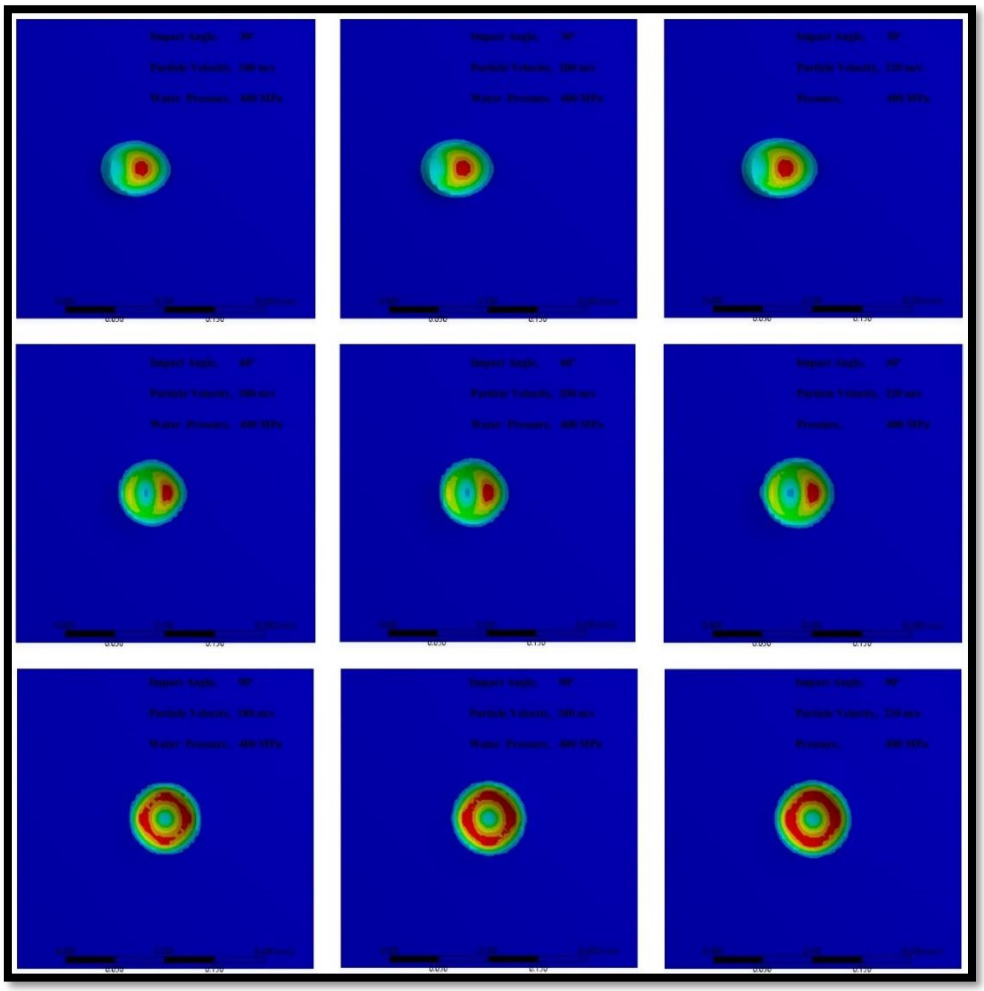

Figure (4-1): Plastic strain after particle impact to the target at Impact angle (30^{o} ,60^{o} ,90^{o}) at water Pressure 400 MPa

From (Figure 4-2 and 4-3), it's noticed that Crater Diameter increased with increasing Travers Rate **T** (Example from 200 m/s 220 m/s) at same Impact Angle **α,** also it's noticed that same effect happened with increasing Water Pressure **P** (From 400 MPa to 600 MPa) at the same other conditions

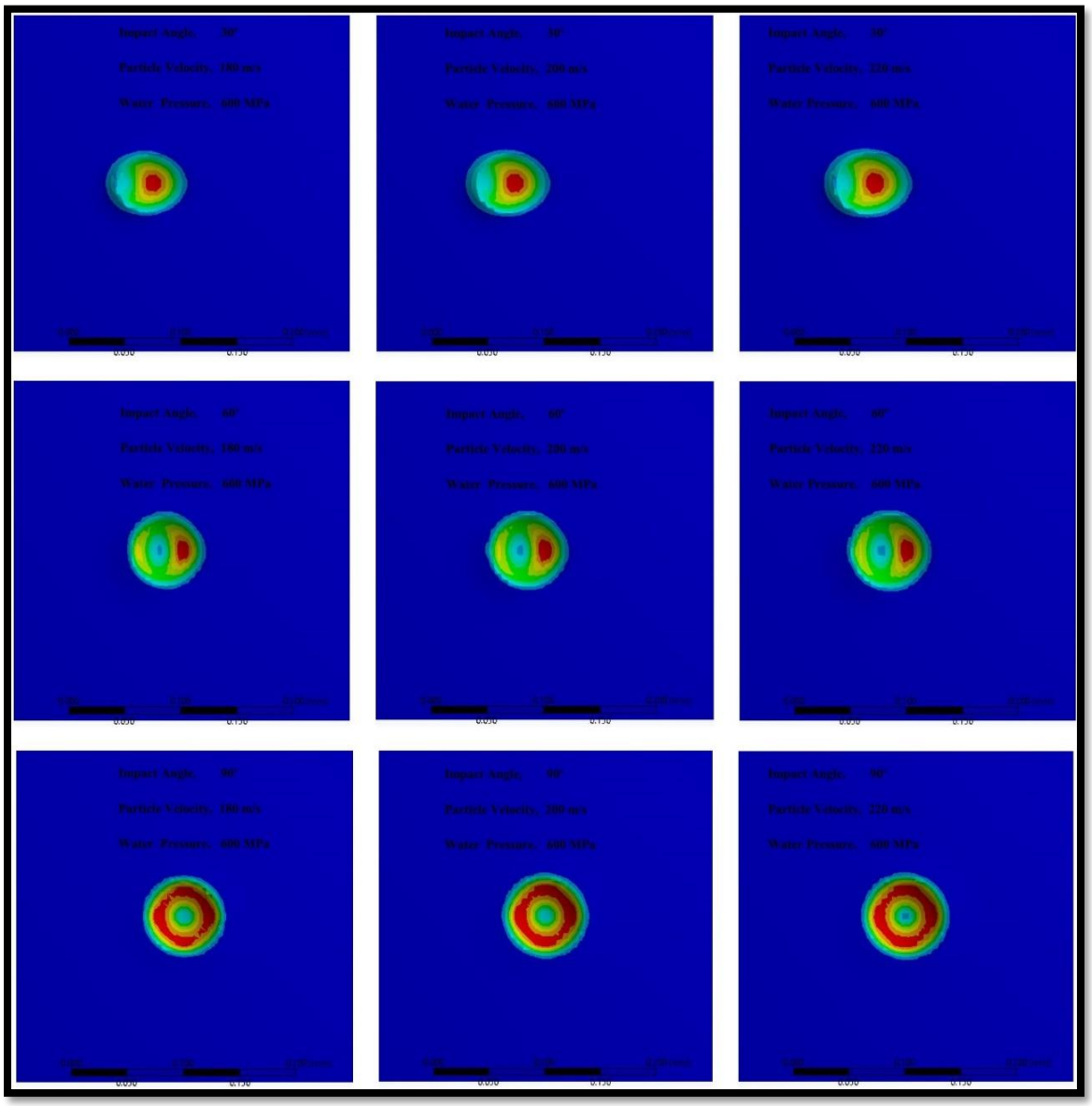

Figure 4-2: Plastic strain after particle impact to the target at impact angle (30^o ,60^o ,90^o) at water Pressure 400 MPa

dimensions calculated from charts that given by ANSYS Software as below (see Figure 4-3):

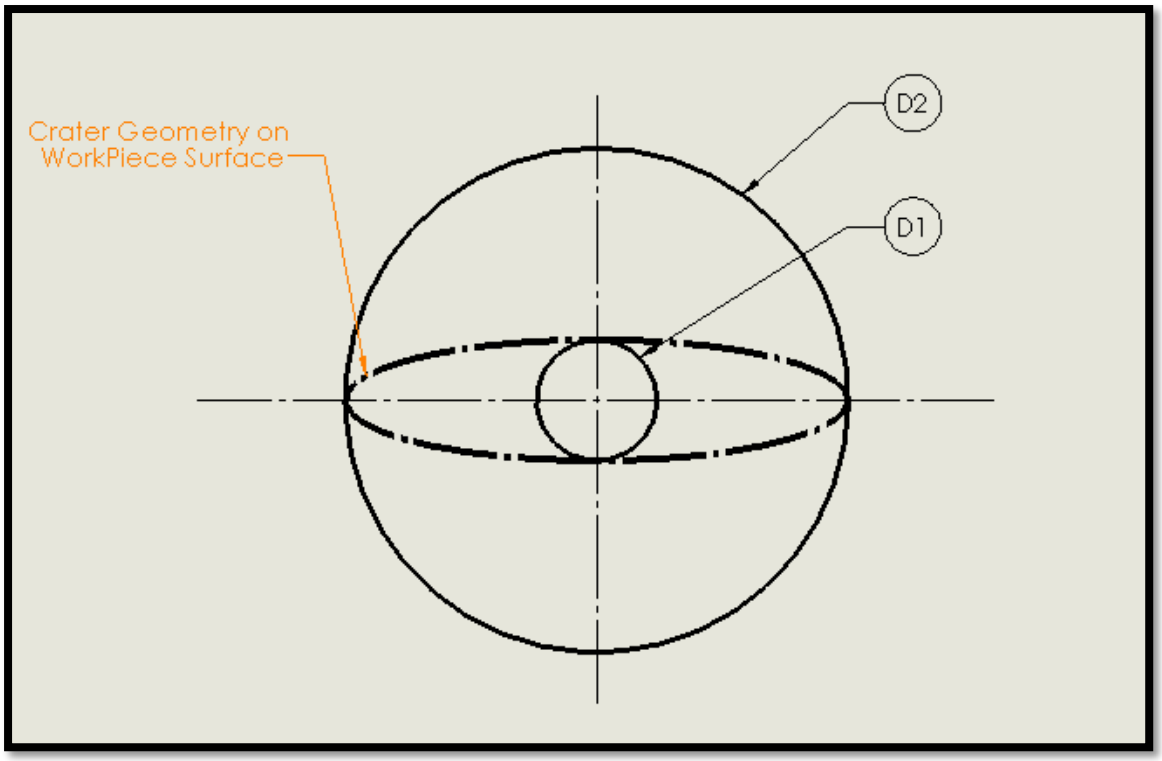

Figure 4-3: Crater circularity definition (D1≡Minor carter diameter), (D2≡Major carter diameter) (C≡ Carter Geometry circularity).

Circularity had been calculated according to equation:

$$C = \frac{D2}{D1} \qquad [20]\ [22]$$

and results came as given below (see Table 4-1):

Table 4-1: Minor carter diameter D_1, Major carter diameter D_2 and circularity C at water Pressure 400 MPa

Water Pressure P = 400 MPa									
Traverse Rate (m/s)	α = 30°			α = 60°			α = 90°		
	$D_{1(mm)}$	$D_{2(mm)}$	$C_{(mm)}$	$D_{1(mm)}$	$D_{2(mm)}$	$C_{(mm)}$	$D_{1(mm)}$	$D_{2(mm)}$	$C_{(mm)}$
T = 180	0.057	0.071	1.24561	0.068	0.069	1.01471	0.072	0.073	1.01389
T = 200	0.059	0.074	1.25424	0.070	0.071	1.01429	0.076	0.077	1.01316
T = 220	0.061	0.077	1.26230	0.072	0.075	1.04167	0.079	0.078	0.98734

Table 4-2: Minor carter diameter D_1, Major carter diameter D_2 and circularity C at water Pressure 600 MPa

Water Pressure P = 600 MPa									
Traverse Rate (m/s)	α = 30°			α = 60°			α = 90°		
	$D_{1(mm)}$	$D_{2(mm)}$	$C_{(mm)}$	$D_{1(mm)}$	$D_{2(mm)}$	$C_{(mm)}$	$D_{1(mm)}$	$D_{2(mm)}$	$C_{(mm)}$
T = 180	0.058	0.074	1.27586	0.069	0.071	1.02899	0.075	0.075	1.00000
T = 200	0.060	0.076	1.26667	0.071	0.075	1.05634	0.079	0.080	1.01266
T = 220	0.062	0.079	1.27419	0.072	0.076	1.05556	0.080	0.080	1.00000

Results from (Tables 4-1 and 4-2) had been charted to show influences of modifying selected Parameters Exactly Impact Degree **α** on Circularity **C** (see Figure 4-4) and (see Figure 4-5).and it's noticed that when impact angle altered from 90^O Circularity Value deviated from 1.00.

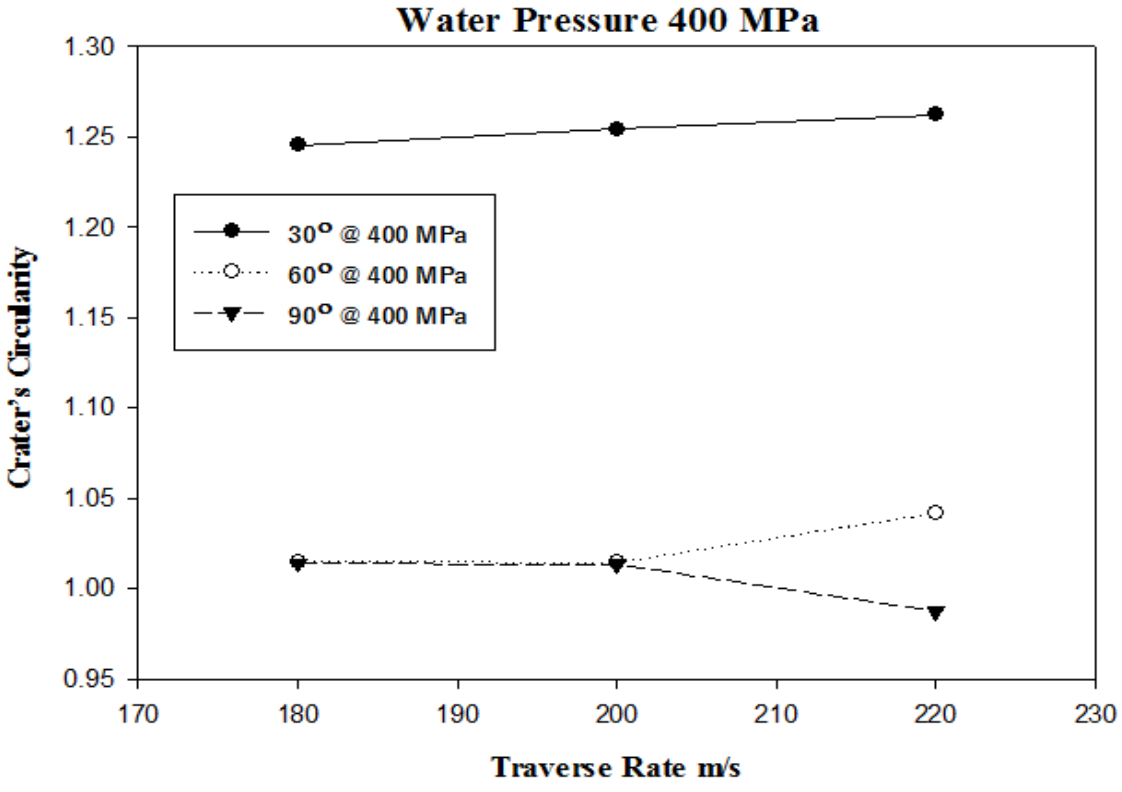

Figure (4-4): Simulated craters circularity as a function of particle velocity and its impact angle at Pressure 400 MPa

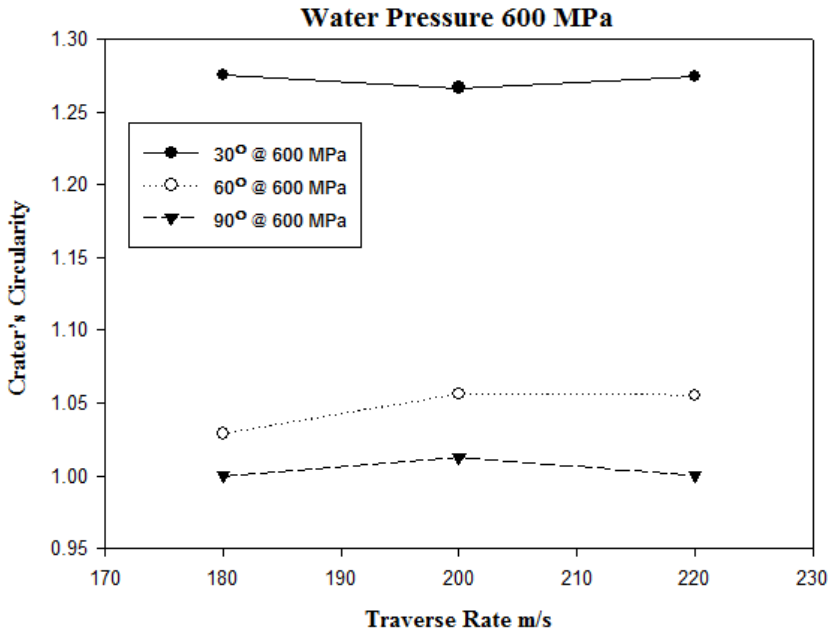

Figure (4-5): Simulated craters circularity as a function of particle velocity and its impact angle at Pressure 600 MPa

4.2 FEA Simulation Results Comparison

From (Figure 4-6) it's Clear that Circularity Value Deviation increase when Water Pressure increased to 600 MPa from 400 MPa.

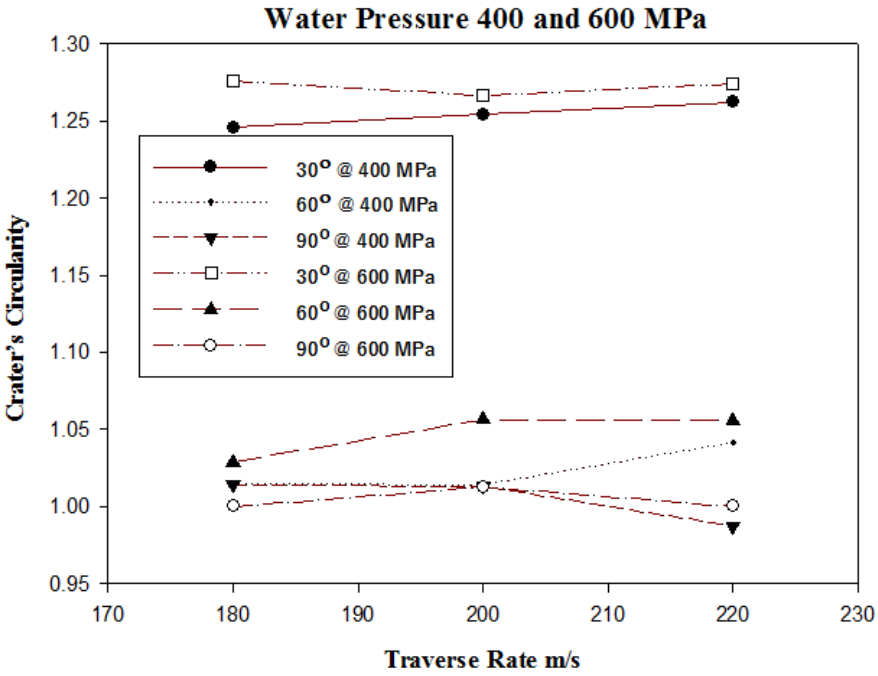

Figure (4-6): Comparison of circularity between 400 MPa and 600 MPa

CHAPTER V

CONCLUSION AND RECOMMENDATION

CHAPTER V

CONCLUSION AND RECOMMENDATION

5.1 FEA Simulation Conclusion:

The work presented here is an overview of recent developments of AWJM and future research directions. The investigation on various process parameters of AWJM showed an increase in Material Removal Rate (MRR) by (1% – 3%) with increasing Water Pressure P by 200MPa and (4% – 5%) approximately with increasing Traverse Rate T by 20m/s, but also showed drawbacks as surface roughness and damage When Impact Angle 90^{O} showed the best results.

5.2 Recommendations:

There are many aspects which could be subject of a research in this field and I hope this research be start whistle for other research. In this research Single particle was used to impact the Workpiece. multi particles, other Impact angles, higher Travers Rates also depth of Crater could be a good topic for Research

REFERENCES

[1] S. K. &. S. R.Schmid, Manufacturing Engineering & Technology (6th Edition), Prentice Hall Professional Technical Ref, 2009.

[2] D. G. D. A. M. M. Korat, "A Review on Current Research and Development in Abrasive Waterjet Machining," *International Journal of Engineering Research and Applications,* vol. 4, no. 1, pp. 423-432, 2014.

[3] M. H. A.A. Khan, "Performance of different abrasive material during abrasive water jet," *Journal of Materials Processing Technology,* vol. 191, pp. 404-407, 2007.

[4] A. A. M.A. Azmir, "A study of abrasive water jet machining process on glass/epoxy," *Journal of Materials ProcessingTechnology,* vol. 209, p. 6168–6173 , 2009.

[5] U. C. a. H. G. ,. Ahmet Hascalik, "Effect of traverse speed on abrasive water jet machining of Ti–6Al–4V alloy," *Materials and Design ,* vol. 28, p. 1953–1957, 2007.

[6] N. R. B. ,. J. John Rozario Jegaraj, "A strategy for efficient and quality cutting of materials with abrasive waterjets considering the variation in orifice and focusing nozzle diameter," *International Journal of Machine Tools & Manufacture,* vol. 45, p. 1443–1450, 2005.

[7] W. W. J. Wang, "A study of abrasive water jet cutting of metallic coated sheet steels," *International Journal of Machine Tools & Manufacture,* vol. 39, p. 855–870, 1999.

[8] Mohemed Hashish, "Observations on cutting with 600-MPa waterjets," *Journel of pressure vessel technology,* vol. 124, 2002.

[9] Hocheng and K.R. Chang, "Material removal analysis in abrasive water jet cutting of ceramic plates," *Journal of Materials Processing Technology,* vol. 40, pp. 287-304, 1994.

[10] Mahabalesh Palleda, "A study of taper angles and material removal rates of drilled holes in the abrasive water jet machining process," *Journal of Materials Processing Technology,* vol. 18, p. 292–295, 2007.

[11] A. S. T. A. G. A. E.-P. K. R. A. Alberdi, "Composite Cutting with Abrasive Water Jet," in *The Manufacturing Engineering Society International Conference*, 2013.

[12] D. S. R. D. M.Chithirai Pon Selvan, "Effects of Process Parameters on Depth of Cut in Abrasive Waterjet Cutting of Cast Iron," *International Journal of Scientific & Engineering Research,* vol. 2, no. 9, 2011.

[13] Autodesk, "Finite Element Analysis," 12 8 2015. [Online]. Available: http://www.autodesk.com/solutions/finite-element-analysis.

[14] D. V. Hutton, Fundamentals of Finite Element Analysis, McGraw-Hill Companies, The.

[15] S. Moaveni, Finite Element Analysis Theory and Application with ANSYS (3rd Edition), Prentice Hall, 2007.

[16] Wikipedia, "ANSYS," Wikipedia, [Online]. Available: https://en.wikipedia.org/wiki/Ansys. [Accessed 23 9 2015].

[17] ANSYS, "ANSYS Advantages," ANSYS, [Online]. Available: http://www.ansys.com/About+ANSYS/ANSYS+Advantages. [Accessed 6 11 2015].

[18] ANSYS, "ANSYS Mechanical," ANSYS, [Online]. Available: http://www.ansys.com/Products/Simulation+Technology/Structural+Analysis/ANSYS+Mechanical. [Accessed 5 12 2015].

[19] ANSYS, "Explicit Dynamics Solutions," ANSYS, [Online]. Available: http://www.ansys.com/Products/Simulation+Technology/Structural+Analysis/Explicit+Dynamics. [Accessed 5 12 2015].

[20] B. J. ,. M. F. ,. M. G. M. Junkar, "Finite element analysis of single-particle impact in abrasive water jet machining," *International Journal of Impact Engineering,* vol. 32, p. 1095–1112, 2006.

[21] Ainnovative, "Abrasive Water Jet Cutting," Ainnovative, [Online]. Available: http://www.ainnovative.co.in/abrasive-water-jet-cutting-434274.html. [Accessed 23 8 2015].

[22] A. A. N. B. Kyriaki Maniadaki, "Effect of impact angle and velocity in crater circularity in abrasive water jet machining by means of multi-particle impact simulation," *Int. J. Machining and Machinability of Materials,* vol. 10, pp. 34 - 47, 2011 .

[23] P. M. D. S. A. Henning, "Efficient Operation of Abrasive Waterjet Cutting in Industrial Applications," in *WJTA-IMCA Conference and Expo* , Houston, Texas, 2011 .

APPENDICES

Figures from [Finite element analysis of single-particle impact in abrasive water jet machining] by [M. Junkara, B. Jurisevica, *, M. Fajdigab, M. Grahc]:

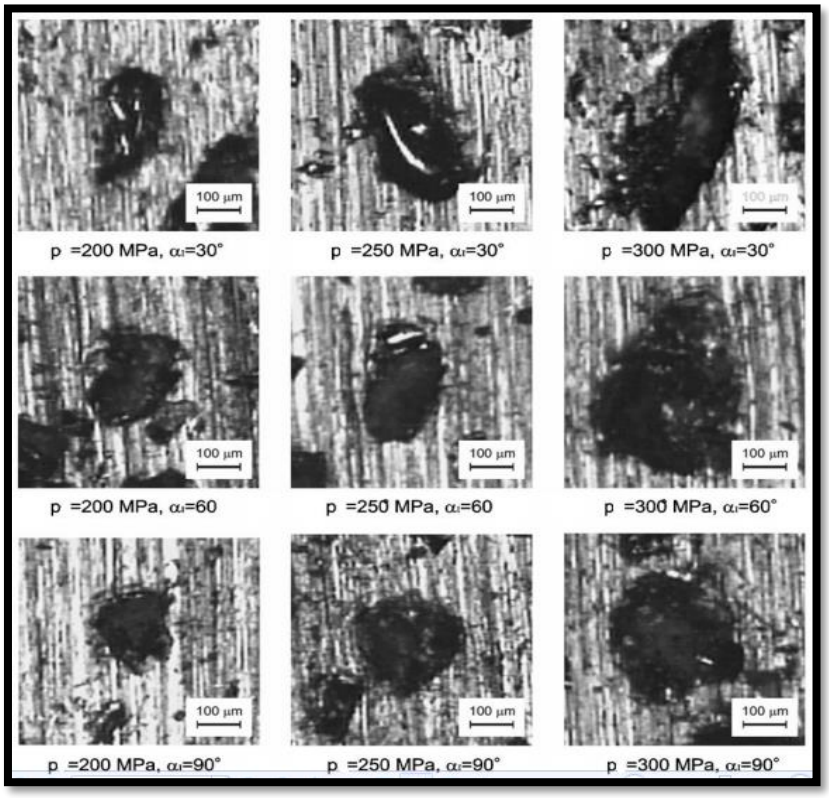

Figure (2-12) Craters made at different water pressures and impact angles

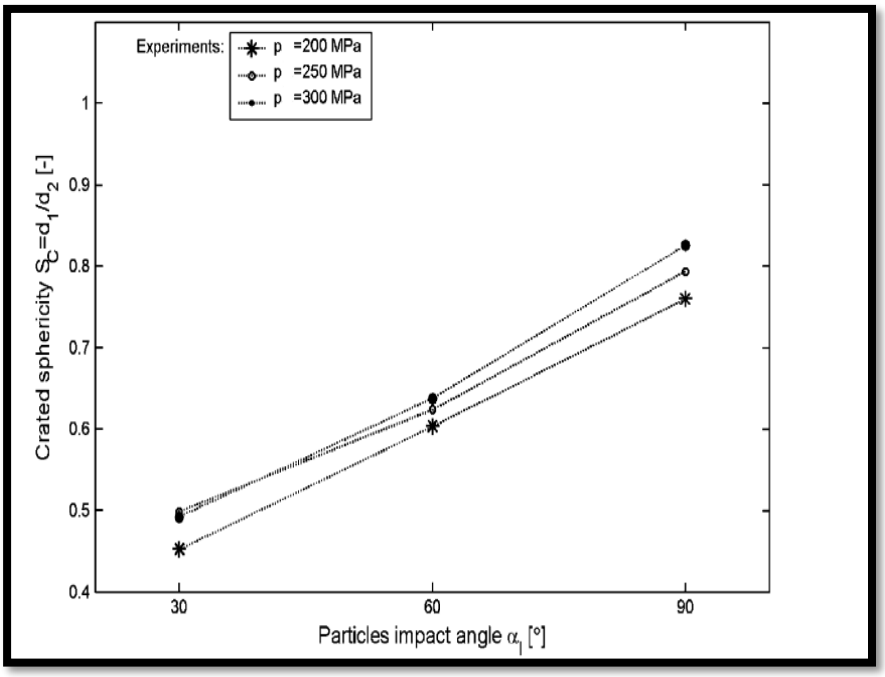

Figure (2-13) Average crater Sphericity as function of impact angle at different water pressures.

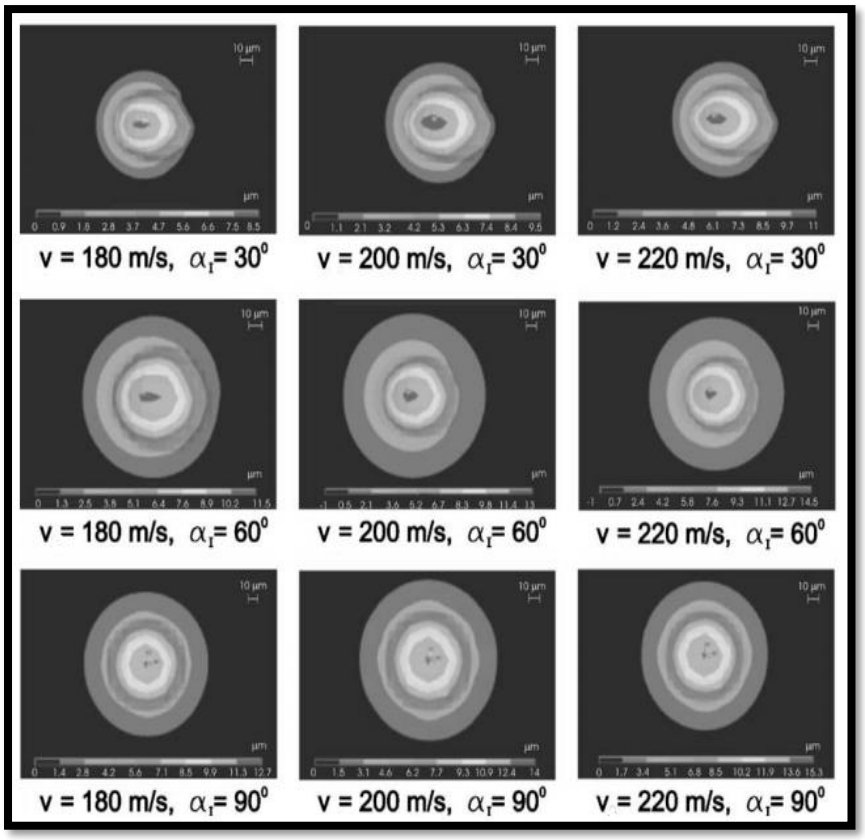

Figure (2-14) Craters simulated at different particle velocities and impact angles.

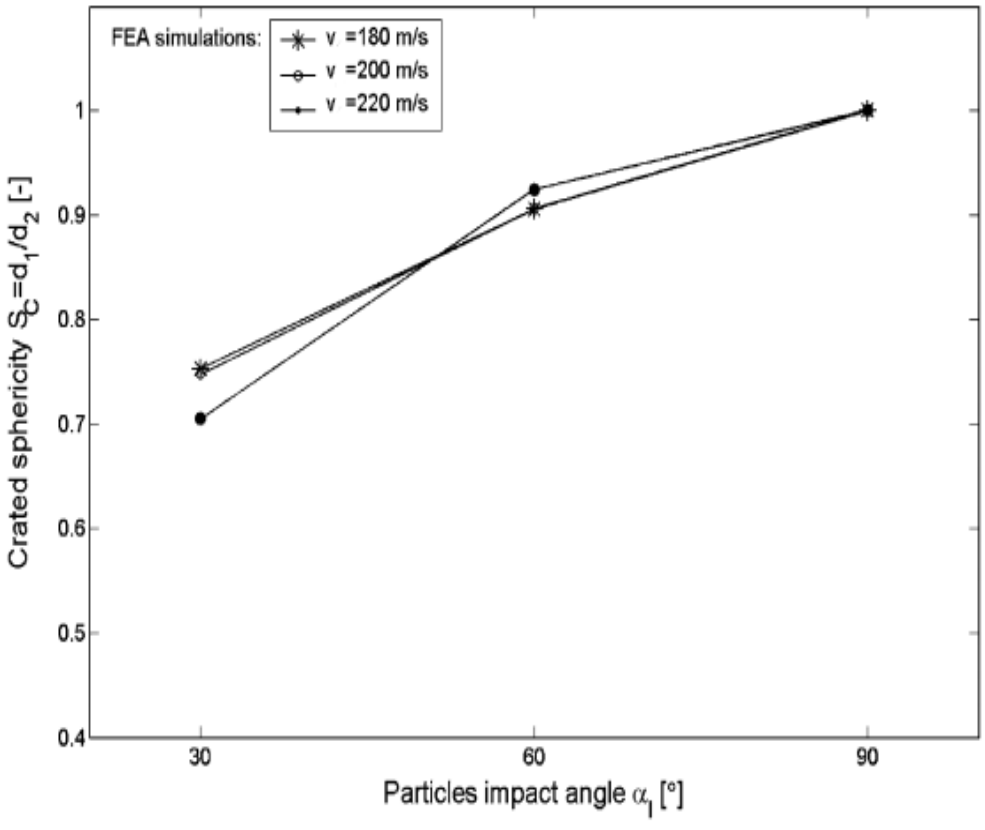

Figure (2-15) Simulated craters Sphericity as a function of particle velocity and its impact angle.

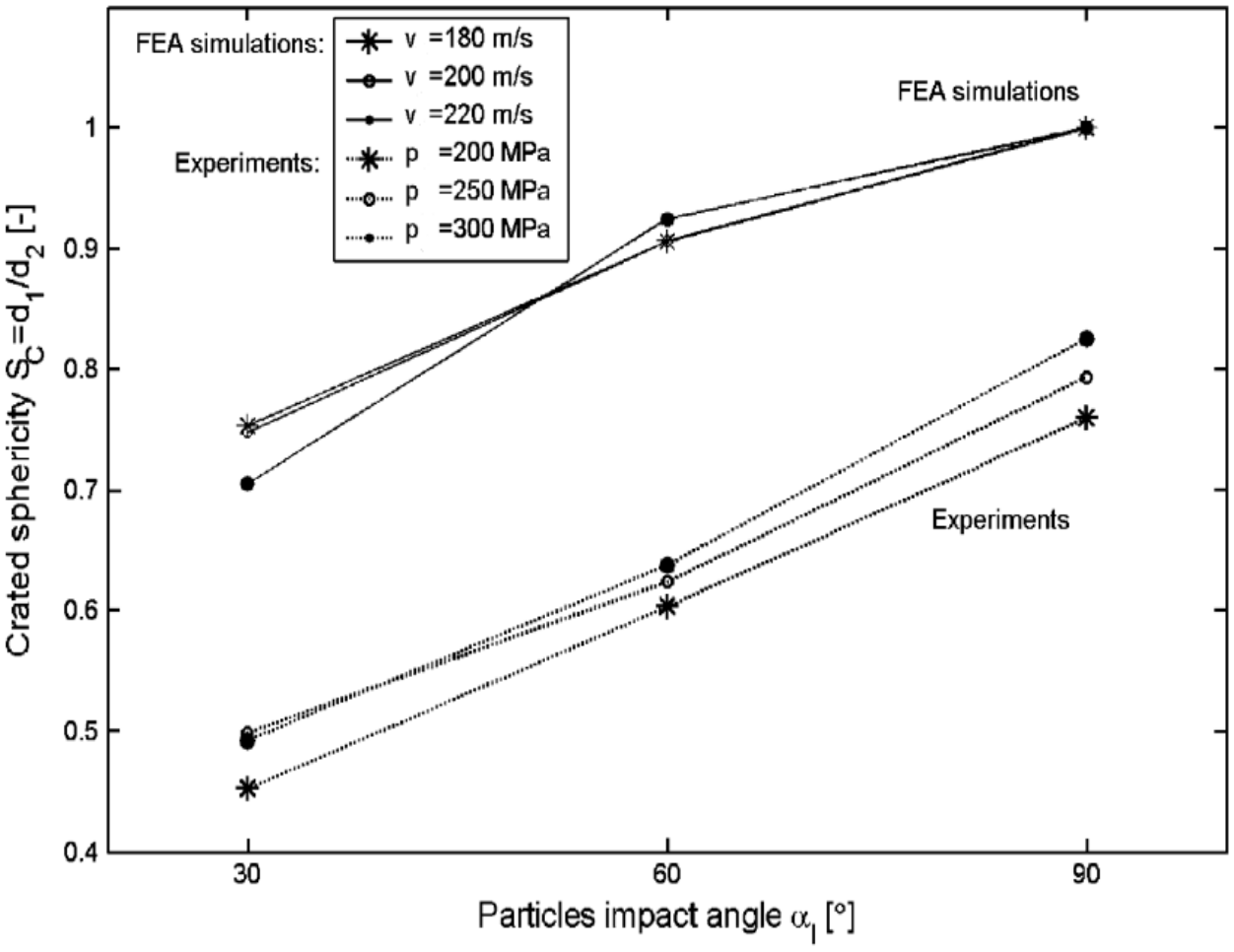

Figure (2-16) Comparison of FEA simulations experimental results.